FEW THEORETICAL REMARKS ON THE DYNAMICAL CONTROL OF RACING SAILING BOATS WITH FOILS

PHILIPPE DESTUYNDER* AND CAROLINE FABRE**

* Département d'ingénierie mathématique, laboratoire M2N
Conservatoire National des Arts et Métiers
292, rue saint Martin, 75003 Paris France
philippe.destuynder@cnam.fr
** Laboratoire de mathématiques d'Orsay, UMR 8628
Univ Paris-Sud, CNRS, Université Paris-Saclay
Orsay 91405 France
caroline.fabre@u-psud.fr

ABSTRACT. The development of foils for racing boats has changed the strategy of sailing. Recently, the America's cup held in San Francisco, has been the theatre of a tragicomic history due to the foils. During the last round, the New-Zealand boat was winning by 8 to 1 against the defender USA. The winner is the first with 9 victories. USA team understood suddenly (may be) how to use the control of the pitching of the main foils by adjusting the rake in order to stabilize the ship. And USA won by 9 victories against 8 to the challenger NZ. Our goal in this paper is to point out few aspects which could be taken into account in order to improve this mysterious control law which is known as the key of the victory of the USA team. There are certainly many reasons and in particular the cleverness of the sailors and of all the engineering team behind this project. But it appeared interesting to have a mathematical discussion, even if it is a partial one, on the mechanical behaviour of these extraordinary sailing boats. The numerical examples given here are not the true ones. They have just been invented in order to explain the theoretical developments concerning three points: the interest of track for sailing upwind, the nature of foiling instabilities when the boat is flying and the control laws on the daggerboard bearing the main foil.

FIGURE 1. Principle of the flying boat with the AC45 of Oracle USA Team

Date: 03-26-2016.
2010 *Mathematics Subject Classification.* Primary: 35C07, 65M15; Secondary: 35M12, 65T60.
Key words and phrases. hydrodynamics of foils, exact control, constrained control, optimal control.

1. **Introduction.** The control of foiling during the America's cup appeared to be a determinant point in the success of Oracle Team USA (OTUSA). In particular during upwind legs, when the boat had to avoid the waves created by the wake of the preceding boat, the automatic stabilisation is a fundamental advantage that OTUSA exploited in a smart way and finally won the competition. Such situations are represented on the figures 2 taken from TV transmissions during the America's cup in San Francisco (September 2013). The analysis of the regulation used by OTUSA is discussed at subsection 6.6.

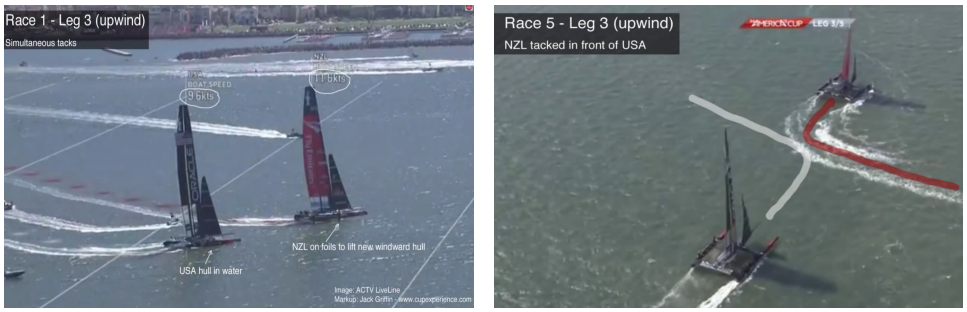

FIGURE 2. Two situations where the controlled foiling could avoid to tack and to loose the race

A slightly more simple algorithm is discussed in subsection 6.5. But the optimal solution which is given in section 6.1 (without upperbound on the amplitude of the rake control) and in 6.4 (with upperbound on the rake control), are more efficient. Unfortunately, it remains to define the mechanical device which enables one to apply these optimal control laws and which are rule compliant. We do not publish here this technological aspect but the method published by OTUSA and which is shown in the annex at the end of this paper, is very close to what can be done. In the section 2 we discuss briefly the apparent wind velocity phenomena which is a general concept and which is also extended in the following to the one of apparent hydraulic velocity for the foils.

In this paper, we have tried to give a more precise mathematical analysis of what can be done using recent tools in the framework of automatic control. But, even if a more industrial 3D analysis is available, and in order to be as simple as possible we restrict our analysis to a bi-dimensional case. Hence only two movements of the ship are taken into account: the heaving which is a normal displacement to the surface of the sea, and the pitching which is the rotation around an axis transverse to the main direction of the ship. Hence, the yawing angle and the rolling are eliminated from our model. Obviously they are meaningful, but according to our mind, not necessary for the understanding of our purpose.

The inclination of the main foil is manually driven even if a hydraulic ram can be used (rules of the race) and because the system is a second order one (with inertia, damping and stiffness), only a phase control can lead to optimal results. This driven angle is named the rake and it is the control variable of our problem. It appears, in the numerical simulations, that the regulation law strongly depends on the ship velocity. In fact, this paper contains four parts. But the main contributions are in the two last ones where we discuss the stall flutter phenomenon of the foils and the influence of the velocity of the ship -say u- on the exact control law of the rake. Even if the experimental data that we introduce in our numerical model could be improved, they are sufficient in order to give an idea of how things work.

As said before, the movement is assumed to be represented by two functions (see figure 3). The heaving z and the pitching angle γ. The equilibrium is written at an arbitrary point -say O. For sake of convenience it is chosen to be the center of rotation of the main foil where is the jack handled by the so-called *Rakeman*[1]. The forces applied to the ship and implying an evolution of these two functions, are those due the rear and the main foils. The local aerodynamical coefficients (c_z for the lift and c_m for the pitching moment) depend respectively on the apparent local angle of attack of each foil. For the rear foil, it is $(\beta+\gamma)_a$ and $(\alpha+\gamma)_a$ for the main one.

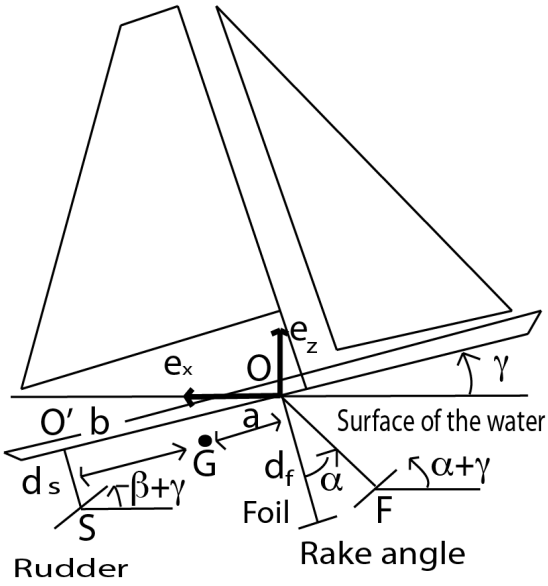

FIGURE 3. Main notations used in the model

The following notations are used:

- M is the mass of the ship;
- J_G is the inertia around the center of mass G, J_O the one at point O and $J_f << J_0$ the one of the main foil at O;
- M_o is the moment of the external forces at point O;
- g is the gravity;
- ϱ_a mass density of the air;
- ϱ_e mass density of the water;
- d_s is the length of the stick supporting the steering rudder;
- d_f is the length of the foil in the depth direction;
- a, b are respectively the distance between the center of mass and O (respectively O'); furthermore $h = a + b$;
- z is the heaving;
- γ is the pitching angle of the ship;
- α is the rake (of the main foil);

[1] in fact he is is the man who adjusts the rake of the main foil

- $c_{zf}, c_{mf}, c_{zs}, c_{ms}$ are the aerodynamical coefficients expressed at point O;
- S_s, S_f are respectively the cross sections of the foils at the extremities of the rudder and the main foil;
- V is the absolute wind velocity;
- V_a is the modulus of the apparent velocity of the wind;
- V_{as}, V_{af} are respectively the apparent velocity at the two foils: one on the rudder and the other one which is main one supported by the daggerboard;
- u is the velocity of the ship;
- d_{og} is the distance from the rotation point of the foil to the center of mass of this foil;
- c_f and ξ are respectively the stiffness and the damping coefficient of the system used for the stabilisation of the main foil.

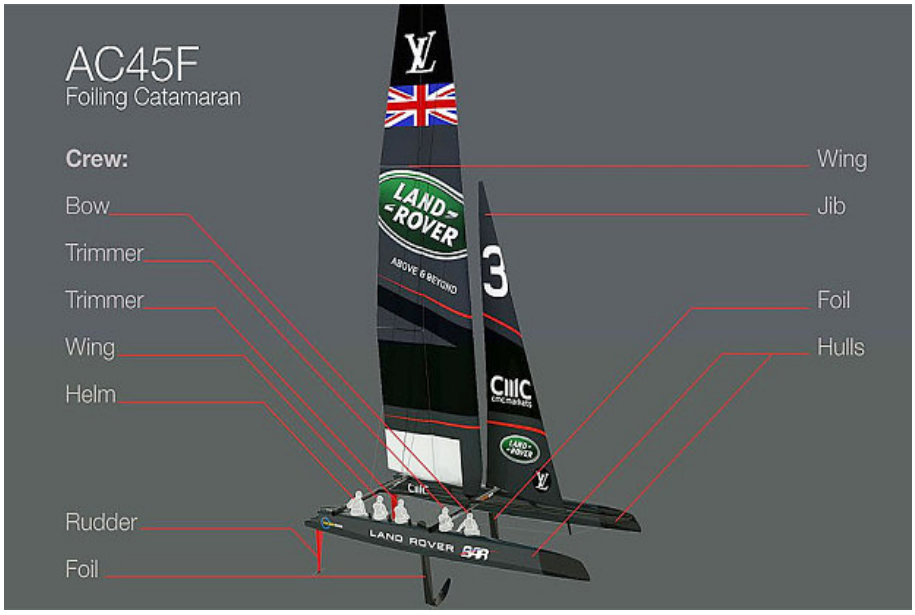

FIGURE 4. Few vocabulary with the britain project AC45 for the 35^{th} challenge.

2. **The apparent velocity of the wind and the overspeed phenomenon.** Even if it is a side subject for our main purpose, it is worth to recall how the apparent wind velocity can induce overspeed for particular positions of the boat with respect to the direction of the wind. The formulae used in this section, aren't really original. Our goal is only to show with a simple numerical simulation, the influence of various parameters on the boat velocity and mainly the one of the sailing position and of the drag coefficient of the bows or the foils in the water.

Let us consider the situation represented on figure 5.

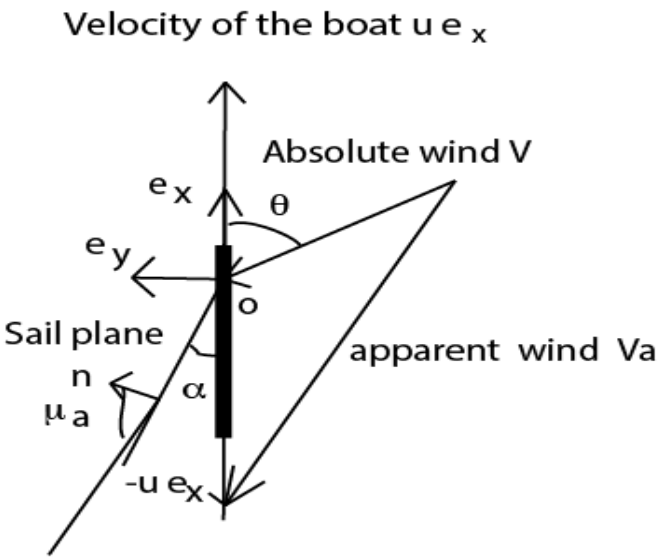

FIGURE 5. The apparent wind and the velocity of the ship

Following the notations of this figure, the apparent wind velocity and the apparent angle between the normal to the sail plane and this apparent wind velocity, are given by:

$$\begin{cases} v_a = -(V\cos(\theta)+u)e_x + V\sin(\theta)e_y, \\ \\ \mu_a = \arccos\left(\dfrac{\sin(\theta-\alpha) - \dfrac{u}{V}\sin(\alpha)}{\sqrt{1+2\dfrac{u}{V}\cos(\alpha)+(\dfrac{u}{V})^2}}\right). \end{cases} \tag{1}$$

The propulsion force due to the wind denoted by F_x, is the projection on the direction e_x of the aerodynamical force applied to the sail. For sake of simplicity it can be written (the square of the $\cos(\mu_a)$ takes into account the normal component of the apparent wind velocity):

$$F_x = \frac{\varrho_a S_a ||V_a||_2^2}{2}\cos(\mu_a)^2\sin(\alpha), \quad (\varrho_a \text{ is the mass density of the air}).$$

In fact, a correction coefficient is included in the surface S_a which takes into account the aerodynamical coefficient $c_z(\mu_a)$ of the sail. The drag force is the sum of two contributions: one due to the sail and another one due to the drag in the water of the bows (zero during the flight) and the foils which are always immersed. Furthermore, the last term depends on both $\beta+\gamma$ and $\alpha+\gamma$. Let us assume that this drag force can be evaluated by (ϱ_e is the mass density of the water):

$$T_x = \frac{\varrho_e S_e u^2}{2} c_{xe},$$

where S_e is the cross section immerged into the water and c_{xe} the corresponding drag coefficient. In fact the important number is the product $S_e c_{xe}$. It is about $1.5\ m^2$ for a ship floating and about $.1\ m^2$ for a flying one as far as the profil of the foils are correctly drawn.

Hence the velocity u of the boat is obtained by solving the equation:

$$F_x - T_x = 0.$$

Due to the complexity of the equations, this can be performed numerically. We have drawn on figures 6 the sign of the function $F_x - T_x$ with respect to the two variables u on the abscissa which is the velocity of the ship and α on the ordinate which is the angle of the sail plane with the direction e_x (velocity of the boat).

The boundary between the two areas are the solutions. The first set of figures (6) corresponds to a floating boat and the two following ones to a flying one. In each case, two figures have been drawn depending on the angle θ between the axis of the boat and the direction of the absolute wind direction as shown on figure 5. In fact they are stationary solutions. Furthermore the data used are realistic but not those corresponding to a racing boat.

For a flying boat, the velocity can be twice the one of the wind an sometimes even more (the expressions depend non linearly of the various parameters).

For the floating boat, it appears, with the set of data used, that the absolute wind velocity can't be overtaken. This is due to the drag force on the bows in the water. In fact the pictures on figures 6 show that a tacking for upwind sailing is much better with large angles concerning the velocity because it enables to make the boat flying above the water using the foils. And even if the distance covered is more important, the time necessary can be smaller. But the flight must be stabilized similarly to what is done with an aircraft. This is more critical if the boat has to cross over the wake of a preceding boat. In fact the phenomenae are very close for a simple reason: the ratio between the aerodynamical forces on the wing of an aircraft is similar to the one applied to the foil of a flying ship. In fact, the ratio between the mass density of the water and the one of the air is about $1000/1.2 \simeq 833$ and the one between the square of the velocities is about $(10/290)^2 \simeq 1/841$. And the equivalence is deduced from the fact that the forces are proportional to the mass density times the square of the velocity.

3. **The apparent flow velocities on the foils.** The apparent velocity of the water on the foils implies the terms $\dot{\gamma}$ and $\dot{z}$. It is the difference between the wind velocity and the one of the boat. First of all let us give the expressions of the velocities of the points S and F corresponding respectively to the rudder and the foil where the hydodynamic forces are given from hydrotunnel tests. One has:

$$\begin{cases} V_s = (\dot{z} - \dot{\gamma}(h\cos(\gamma) - d_s\sin(\gamma)))e_z - \dot{\gamma}(h\sin(\gamma) + d_s\cos(\gamma))e_x), \\ \\ V_f = (\dot{z} + \dot{\gamma}d_f\sin(\alpha+\gamma))e_z - \dot{\gamma}d_f\cos(\alpha+\gamma)e_x. \end{cases} \tag{2}$$

The computations of the hydrodynamic apparent velocities are performed at points S et F in the axis (e_x, e_z) as shown on figure 1. These apparent flow velocities are defined as the difference between the absolute wind velocity -say Ve_x- and the one of the point considered. But let us underline that this so-called (in this paper) where V is the apparent wind velocity as discussed in section 2. Hence there are two different notions for the apparent velocity: the one of the wind and the one of the hydrodynamic flow on the foils. From now on, it is the second one which is taken under consideration. It is given by the

For the floating boat (bows in the water):
$SCX_e = .3\ m^2,\ V = 20m/s\ \theta = .67rd = 38^0\ (left),\ \theta = 1.03rd = 59^0\ (right)$

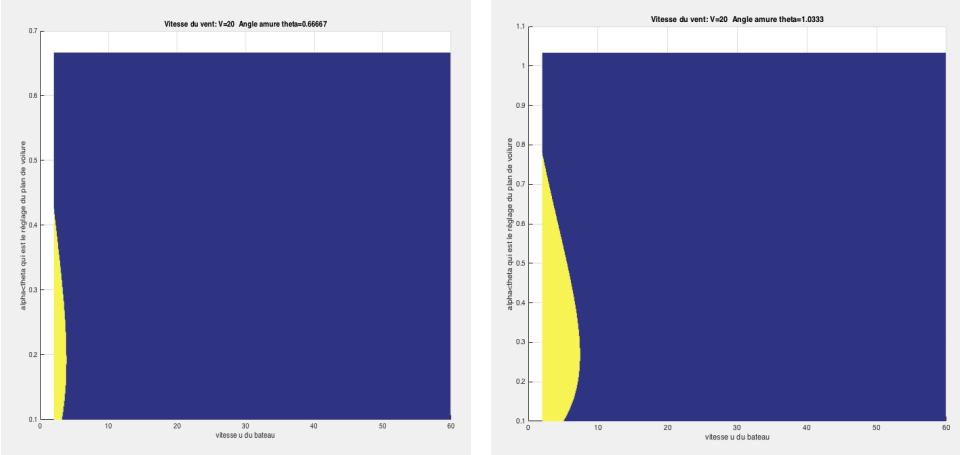

For the flying boat:
$SCX_e = .01\ m^2,\ V = 10\ m/s,\ \theta = .67rd, (left)\ \theta = 1.03rd(right)$

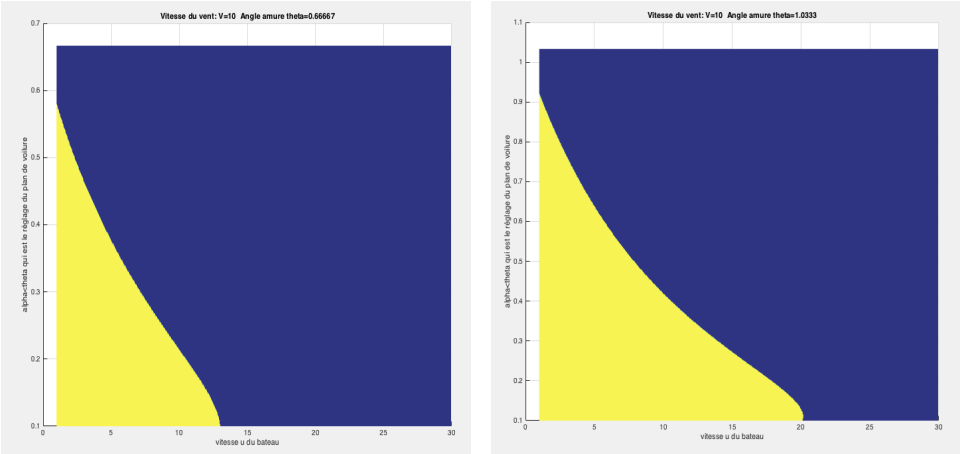

For the flying boat:
$SCX_e = .01\ m^2,\ V = 20\ m/s\ \theta = .67rd\ (left),\ \theta = 1.03\ (right)$

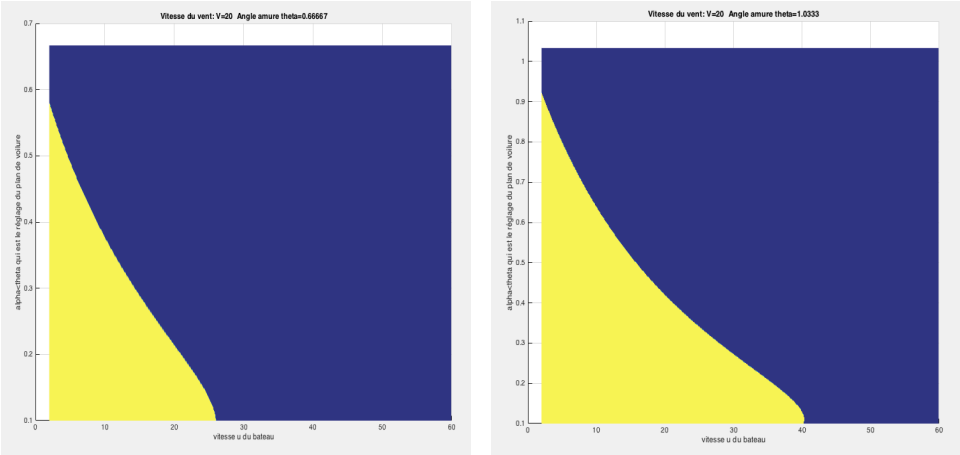

FIGURE 6. Solutions of the equation $F_x - T_x = 0$. The boundaries between the two areas are the solutions. One can see that the ship velocity can be up to $2V$ for $\theta = 59^0\ (= 1.03rd)$. Data used: $\varrho_e = 1000\ kg/m^3,\ \varrho_a = 1.3\ kg/m^3,\ S_a = 900\ m^2$

following formulae where V is therefore the apparent wind velocity:

$$\begin{cases} V_{as} = ue_x - V_s \\ = (u + \dot{\gamma}(h\sin(\gamma) + d_s\cos(\gamma)))e_x - (\dot{z} - \dot{\gamma}(h\cos(\gamma) - d_s\sin(\gamma)))e_z, \\ \\ V_{af} = ue_x - V_f \\ = (u + \dot{\gamma}d_f\cos(\gamma+\alpha)))e_x - (\dot{z} + \dot{\gamma}d_f\sin(\gamma+\alpha))e_z. \end{cases} \tag{3}$$

Furthermore the hydrodynamic apparent angle of attack of both the extremity of the rudder and the one of the driven foil are given by the following expressions $((.,.)$ is the scalar product in $\mathbb{R}^3)$:

$$\begin{cases} (\beta+\gamma)_a = \text{arsin}(\dfrac{(e_y, V_{as} \wedge (\cos(\beta+\gamma)e_x - \sin(\beta+\gamma)e_z))}{|V_{as}|}) \\ \\ (\alpha+\gamma)_a = \text{arsin}(\dfrac{(e_y, V_{af} \wedge (\cos(\alpha+\gamma)e_x - \sin(\alpha+\gamma)e_z))}{|V_{af}|}). \end{cases} \tag{4}$$

The equations of the movement are the following ones (the righthandside is derived from the factor of $\dot{z}$ and $\dot{\gamma}$ in the expression of the power of the hydrodynamical forces):

$$\begin{cases} M\ddot{z} - aM\cos(\gamma)\ddot{\gamma} = \\ \\ \qquad -Mg + \dfrac{\varrho_e S_s |V_{as}|^2}{2} c_{zs}((\beta+\gamma)_a) + \dfrac{\varrho_e S_f |V_{af}|^2}{2} c_{zf}((\alpha+\gamma)_a), \\ \\ -aM\cos(\gamma)\ddot{z} + J_0\ddot{\gamma} = -\dfrac{\varrho_e S_s(h\cos(\gamma) - d_s\sin(\gamma))|V_{as}|^2}{2} c_{zs}((\beta+\gamma)_{as}) \\ \\ + \dfrac{\varrho_e S_f d_f \sin(\alpha+\gamma)|V_{af}|^2}{2} c_{zf}((\alpha+\gamma)_{af}) - M_0 \\ \\ \qquad + \dfrac{\varrho_e S_s L|V_{as}|^2}{2} c_{ms}((\beta+\gamma)_a) + \dfrac{\varrho_e S_f L|V_{af}|^2}{2} c_{mf}((\alpha+\gamma)_a). \end{cases} \tag{5}$$

If the point O were the center of hydrodynamic forces, then one would have $M_0 = 0$. First of all, let us characterize the equilibrium position of the ship. The term (α_0, β_0) corresponding to the equilibrium of the ship over the water ($\gamma = 0$) is solution of:

$$\begin{cases} S_s c_{zs}(\beta_0) + S_f c_{zf}(\alpha_0) = \dfrac{2Mg}{\varrho_e u^2}, \\ \\ -\dfrac{S_s h}{L} c_{zs}(\beta_0) + \dfrac{S_f d_f \sin(\alpha_0)}{L} c_{zf}(\alpha_0) \\ \\ \qquad + S_s c_{ms}(\beta_0) + S_f c_{mf}(\alpha_0) = \dfrac{2M_0}{\varrho_e L u^2}. \end{cases} \tag{6}$$

The solution method of these two coupled equations is easy as far as the coefficients c_{zs}, c_{zf}, c_{ms} and c_{mf} are known. Nevertheless it is worth noting that (α_0, β_0) should be adjusted with the velocity of the wind minus the one of the ship. For example let us set

in the vicinity of $\beta_0,\ \alpha_0$ and $\gamma = 0$ ($\xi_1 = \alpha + \gamma - \alpha_0,\ \xi_2 = \beta + \gamma - \beta_0$):

$$\left\{\begin{array}{l} \text{for } \xi_1 \text{ and } \xi_2 \text{ small enough, we set:} \\ \\ c_{zs}(\beta_0+\xi_2) = c_{zs}(\beta_0) + R_{zs}\xi_2,\ c_{zf}(\alpha_0+\xi_1) = c_{zf}(\alpha_0) + R_{zf}\xi_1, \\ \\ c_{ms}(\beta_0+\xi_2) = c_{ms}(\beta_0) + R_{ms}\xi_2,\ c_{mf}(\alpha_0+\xi_1) = c_{mf}(\alpha_0) + R_{ms}\xi_1. \\ \\ \text{Let us introduce the hydrodynamical stiffness (no apparent velocity) :} \\ \\ R_1 = \dfrac{S_s R_{zs}}{2} + \dfrac{S_f R_{zf}}{2}, \\ \\ R_2 = -\dfrac{S_s h R_{zs}}{2} + \dfrac{S_f d_f \sin(\alpha_0) R_{zf}}{2} + \dfrac{S_s L R_{ms}}{2} + \dfrac{S_f L R_{mf}}{2}. \end{array}\right. \tag{7}$$

4. **Static stability of the flight.** The first point is to discuss the static stability of this solution (α_0, β_0). From equation (5) the stability depends on the real parts of the solution μ of the following equation (let us recall that from Huyghens theorem, one has the relation:

$$J_G = J_0 - a^2\cos(\gamma)^2 M = J_0 - a^2 M,$$

because we study the stability around $\gamma = 0$:

$$\det \begin{vmatrix} -\mu^2 M, & \mu^2 aM - u^2 \varrho_e R_1 \\ \\ \mu^2 aM, & -\mu^2 J_0 - u^2 \varrho_e R_2 \end{vmatrix} = 0. \tag{8}$$

Or else:

$$\mu^2(\mu^2 J_G + \varrho_e u^2 M(aR_1 + R_2)) = 0.$$

The values $\mu = 0$ corresponds to the metastable equilibrium of the ship over the water. It is assumed that this equilibrium is controlled by the velocity of the boat during the flight, mainly by adjusting the rudder which enables to drive slightly the apparent wind velocity. The other solutions are (see figure 7):

$$\mu = \pm i\ u\sqrt{\frac{\varrho_e M(aR_1 + R_2)}{J_G}}.$$

One can observe on figures 7 and 8, that the frequencies are growing with the velocity for a first set and decreasing for another one. But in both cases the values are similar, around $1.5\ Hz$ for the pitching mode (and 0 for the heaving). This is a regular conclusion as far as we choose very simple linear and increasing expressions of the aerodynamical coefficients. But this could depend also on the position of the centre of rotation and the one of the center of mass that we positioned approximatively.

They are pure imaginary numbers as far as $aR_1 + R_2 > 0$ which is a realistic case as far as the pitching angle γ, the inclination of the rear foil β_0 and the control variable α_0 are small enough. This is the case of the regular flight. Furthermore, the fact that $a > 0$ which means that the the center of mass G is slightly behind o is a securing situation concerning the stability. In fact such boatS are built in order to be stable in static. Let us notice that the center of thrust of the wind force is also slightly forward of the center of mass G in order to have a weather helming boat. Finally, the static stability of the ship is ensured as soon as it is correctly built. The real problem will be the dynamic stability at high speed and the stabilisation of the flight when crossing the wake of another ship in order to avoid taking as shown on figure 2.

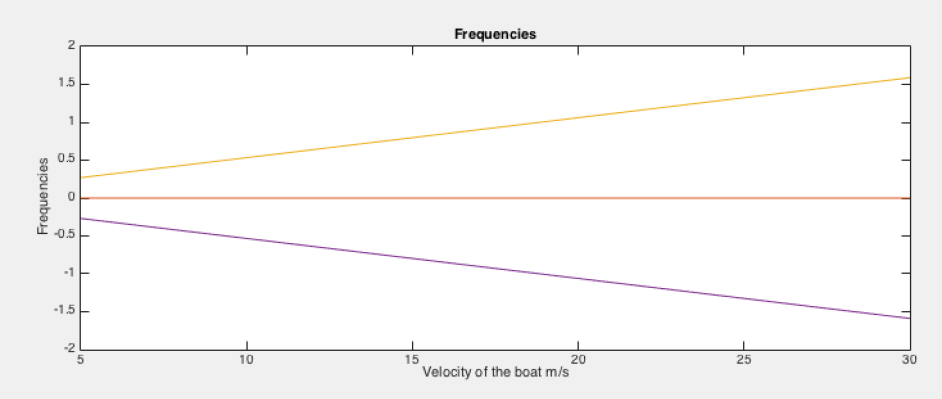

FIGURE 7. The evolution of $\mu/2\pi$ versus the velocity of the boat for a set of foil and rudder

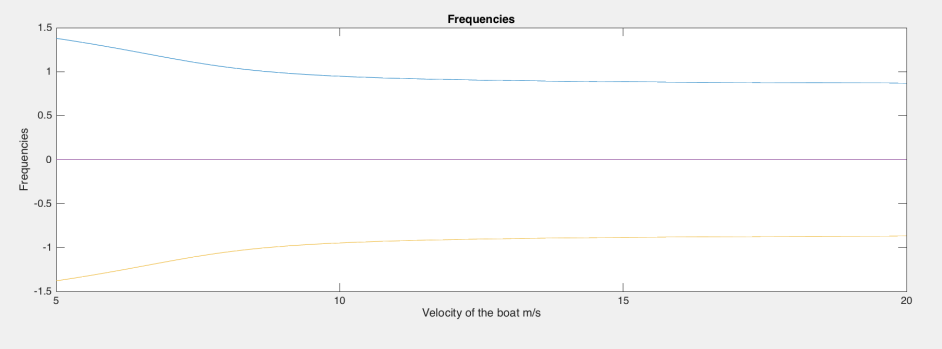

FIGURE 8. The evolution of $\mu/2\pi$ versus the velocity of the boat with another set of foil and rudder

5. **Discussion about dynamical stability.** The discussion on the dynamical stability will be organized from a linearization of these equations around α_0, β_0 solution of (6). The variables are z and γ. Hence, the first step is to formulate the linearized model around an equilibrium position solution of (6). In fact β_0 is assumed to be fixed, and the evolution of the pitching angle of the rear foil is only due to the global pitching of the boat -say γ. In a formal way one can write this linear model as follows:

$$\begin{cases} M\ddot{z} - aM\cos(\gamma)\ddot{\gamma} = u^2\varrho_e R_1\gamma + C_{11}\dot{z} + C_{12}\dot{\gamma}, \\ -aM\cos(\gamma)\ddot{z} + J_0\ddot{\gamma} = u^2\varrho_e R_2\gamma + C_{21}\dot{z} + C_{22}\dot{\gamma}. \end{cases} \tag{9}$$

But in practice, the coefficients $C_{11},\ C_{12},\ C_{21}$ and C_{22} can be computed using a symbolic computation software if for instance a three dimensional modelling would be concerned. In our two dimensional case it is still possible to perform a hand computation. The expressions are given in the tables 1 and 2.

Coefficient	Expression of $\mathcal{C}$
C_{11}	$\varrho_e \dfrac{\partial(S_s\lvert V_{as}\rvert^2 c_{zs}((\beta+\gamma)_a) + S_f\lvert V_a f\rvert^2 c_{zf}((\alpha+\gamma)_a))}{2\,\partial\dot{z}}$
C_{12}	$\varrho_e \dfrac{\partial(S_s\lvert V_{as}\rvert^2 c_{zs}((\beta+\gamma)_a) + S_f\lvert V_{af}\rvert^2 c_{zf}((\alpha+\gamma)_a))}{2\,\partial\dot{\gamma}}$
C_{21}	$-\varrho_e \dfrac{\partial(S_s(h\cos(\gamma) - d_s\sin(\gamma))\lvert V_{as}\rvert^2 c_{zs}((\beta+\gamma)_a))}{2\partial\dot{z}}$ $+\varrho_e \dfrac{\partial(S_f\lvert V_{af}\rvert^2 d_f\sin(\alpha+\gamma)c_{zf}((\alpha+\gamma)_a))}{2\partial\dot{z}}$ $+\varrho_e \dfrac{\partial(S_s L\lvert V_{as}\rvert^2 c_{ms}((\beta+\gamma)_a) + S_f L\lvert V_a f\rvert^2 c_{mf}((\alpha+\gamma)_a))}{2\,\partial\dot{z}}$
C_{22}	$-\varrho_e \dfrac{\partial(S_s(h\cos(\gamma) - d_s\sin(\gamma))\lvert V_{as}\rvert^2 c_{zs}((\beta+\gamma)_a))}{2\partial\dot{\gamma}}$ $+\varrho_e \dfrac{\partial(S_f\lvert V_{af}\rvert^2 d_f\sin(\alpha+\gamma)c_{zf}((\alpha+\gamma)_a))}{2\partial\dot{\gamma}}$ $+\varrho_e \dfrac{\partial(S_s L\lvert V_{as}\rvert^2 c_{ms}((\beta+\gamma)_a) + S_f L\lvert V_a f\rvert^2 c_{mf}((\alpha+\gamma)_a))}{2\,\partial\dot{\gamma}}$

Table 1 Expressions of the coefficients of the matrix $\mathcal{C}$ with respect to $\dot{z}$ and $\dot{\gamma}$

Let us give a more explicit expession of these terms. First of all, one has from a simple analytic computation at the point $\gamma = \dot{\gamma} = \dot{z} = 0$ in the following array (Table 2).

$$\begin{cases} \dfrac{\partial(\beta+\gamma)_a}{\partial\dot{z}} = -\dfrac{1}{u}, \ \dfrac{\partial\lvert V_{as}\rvert^2}{\partial\dot{z}} = 0, \\ \dfrac{\partial(\beta+\gamma)_a}{\partial\dot{\gamma}} = \dfrac{h}{u}, \ \dfrac{\partial\lvert V_{as}\rvert^2}{\partial\dot{\gamma}} = 2ud_s, \ \dfrac{\partial\lvert V_{as}\rvert}{\partial\dot{\gamma}} = d_s, \\ \dfrac{\partial(\alpha+\gamma)_a}{\partial\dot{z}} = -\dfrac{1}{u}, \ \dfrac{\partial\lvert V_{af}\rvert^2}{\partial\dot{z}} = 0, \\ \dfrac{\partial(\alpha+\gamma)_a}{\partial\dot{\gamma}} = -\dfrac{d_f\sin(\alpha_0)}{u}, \\ \dfrac{\partial\lvert V_{af}\rvert^2}{\partial\dot{\gamma}} = 2ud_f\cos(\alpha_0), \ \dfrac{\partial\lvert V_{af}\rvert}{\partial\dot{\gamma}} = d_f\cos(\alpha_0). \end{cases} \tag{10}$$

Hence the expressions of the coefficients C_{ij} are:

Coefficient	Expression of the coefficients of the matrix $\mathcal{C}$ around $\gamma = 0$
C_{11}	$-\frac{\varrho_e u}{2}\big[S_s\frac{\partial c_{zs}}{\partial\beta}(\beta) + S_f\frac{\partial c_{zf}}{\partial\alpha}(\alpha)\big]$
C_{12}	$\frac{\varrho_e u}{2}\big[S_s(2d_s c_{zs}(\beta) + h\frac{\partial c_{zs}}{\partial\beta}(\beta)) + S_f(2d_f c_{zf}(\alpha) - d_f\sin(\alpha)\frac{\partial c_{zs}}{\partial\alpha}(\alpha))\big]$
C_{21}	$\frac{\varrho_e u}{2}\big[S_s h\frac{\partial c_{zs}}{\partial\beta}(\beta) - S_f d_f\sin(\alpha)\frac{\partial c_{zf}}{\partial\alpha}(\alpha) - L\big[S_s\frac{\partial c_{ms}}{\partial\beta}(\beta) + S_f\frac{\partial c_{mf}}{\partial\alpha}(\alpha)\big]\big]$
C_{22}	$-\frac{\varrho_e S_s h u}{2}[2d_s c_{zs}(\beta) + h\frac{\partial c_{zs}}{\partial\beta}(\beta)] + \frac{u S_f d_f^2}{2}[\sin(2\alpha)c_{zf}(\alpha) - \sin(\alpha)^2\frac{\partial c_{zf}}{\partial\alpha}]$ $+\frac{\varrho_e u L S_s}{2}\big[2d_s c_{ms}(\beta) + h\frac{\partial c_{ms}}{\partial\beta}(\beta)\big]$ $-\frac{\varrho_e u L}{2}S_f d_f\big[\sin(\alpha)\frac{\partial c_{mf}}{\partial\alpha}(\alpha) + 2\cos(\alpha)c_{mf}(\alpha)\big]$

Table 2 Expressions of the coefficients C_{ij} around $\gamma = 0$ versus α and β

As an example for a symmetrical NACA airfoil one has approximatively in the vicinity of $\alpha \simeq 0$ (α is in radian):

$$C_z(\alpha) = 7\alpha, \qquad C_m(\alpha) = 1.15\alpha \text{ at point of fixation } S \text{ or } F). \tag{11}$$

5.1. **Dynamic stability of the flight.** There are four kind of dynamic instabilities which can occur in general.

1. One is well known by the sailors. It concerns induced vibrations on the rudder due to vortices created by the main foil. But, this so called buffting [6] [**?**] effect, can occur only for very particular cases. In our case it would be due to a vortex shedding from the main foil onto the one of the rudder. And it would appear if the frequency of the vortices is close to the one of the rudder and its foil. It is quickly detected and should be suppressed by an ad'hoc conception of the ship. It is not necessarily destroying but can reduce the efficiency considerably as far as it takes energy from the kinetical energy of the boat.
2. The second one is the classical flutter which is violent and corresponds usually to the unlimited exchange of energy between two movements with the same eigenfrequencies (here the heaving and the pitching). Clearly the secure flight of a ship would be seriously compromised by such an instability implying an exponential increase of the movement of the ship [23]. It would be difficult to control it using the main

foil without additional lifting supplementary wing. Furthermore, because the phenomenon is very quick and complex, its control requires an automatic loop driven by an electronic computer [22]. Because the movement is very quick and complex. In fact as far as the boat is flying over the water, there no stiffness on the heaving excepted the one due to the hydrodynamical forces acting on the foils which are fully immersed in our model. May be it would be different if the bows were in contact with the water and the *Archimède* forces would operate.

3. The third possibility of instability is due to a fluctuation of the wind velocity. It is a rather complex phenomena implying the apparent wind velocity which is under the skipper control. It is discussed in section 2. It could be compared from the mathematical point of view to the buffting phenomena but it is fully different from the mechanical point of view.
4. The fourth dynamical instability and last in our discussion, is due the apparent water velocity on the foils. It could be compared to a stall flutter phenomena as the one encountered in the breakdown of the famous Tacoma-Narrows bridge which fall down in November 1940. This accident was correctly explained forty years later by R. Scanlan [21]. See also [20] for a similar collapse of a model of a military aircraft. In the case of the flying boats this is discussed in section 3.

The stability is governed by the real part of the eigenvalues μ solution of:

$$\begin{vmatrix} -M\mu^2 - i\mu C_{11}, & aM\cos(\gamma)\mu^2 - i\mu C_{12} - u^2\varrho_e R_1 \\ aM\cos(\gamma)\mu^2 - i\mu C_{21}, & -J_0\mu^2 - i\mu C_{22} - u^2\varrho_e R_2 \end{vmatrix} = 0 \qquad (12)$$

By expliciting the previous determinant, one obtains (the classical instabilities are those detected around the equilibrium position such that $\gamma = 0$):

$$\begin{cases} \mu^4 M J_G + i\mu^3(C_{11}J_0 + C_{22}M + a(C_{12}+C_{21})M) \\ +\mu^2[u^2\varrho_e M(R_2 + aR_1) + C_{12}C_{21} - C_{11}C_{22}] \\ i\mu(u^2\varrho_e(C_{11}R_2 - C_{22} - C_{21}R_1)) = 0. \end{cases} \qquad (13)$$

In fact, the coefficients $R_1, R_2, C_{11}, C_{12}, C_{21}$ and C_{22}, depend on the velocity u of the ship. Therefore, the instabilities can appear from two possibilities concerning the ship velocity.

1. *One of the solutions in μ (which are real for $u = 0$) becomes imaginary and therefore one with a negative real part leads to an exponential instability. This is a so-called stall flutter phenomenon.*
2. *The other possibility appears when the solutions are double. Then necessarily a flutter phenomenon is starting.*

The evolution of the solution in μ have been plotted on figure 9 for some particular values of the coefficients.

6. **The control of dynamical behavior via the rake of the main foil.** There are two steps: the first one consists in defining an exact control without constraint and the second step takes into account the constraints on the control magnitude. In this second step appears the links between the control time -say T- and the bounds on the magnitude of the control (ie. the maximum of the magnitude of the rake).

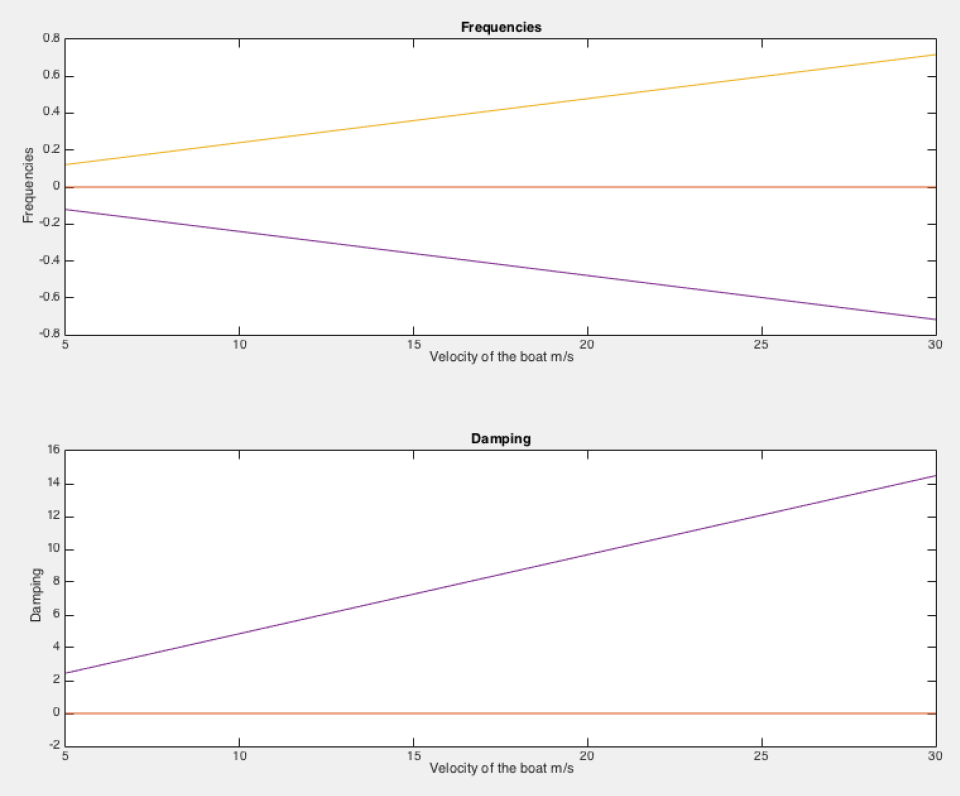

FIGURE 9. The eigenvalues of the dynamical system versus the velocity of the ship

6.1. **The control without constraint.** The control variable is the rake α. In this study we don't discuss the pratical feasibility of the optimal control law that we compute. It is just an indication of what should be done and it can be understood as an educational result, as far as the real driven law is manual. The strategy that we are using consist in defining a control criterion and to minimize it with respect to the control variable. This control criterion is a norm of the gap between the observed state variables at a time T (pitching and heaving) and the desired values of these functions. Furthermore we make use of a linearized approximation of the state equation.

Therefore the control problem consists in defining a criterion depending on the state variables (ie. z and γ) but also on the control $\delta = \alpha - \alpha_0$ and to minimize it with respect to δ. Let us first define a delay -say T- corresponding to the reaction time required in the control process. Our goal is to define a control law such that at time T the ship is back to the equilibrium

$$z(T) = z_0,\ \dot{z}(T) = \gamma(T) = \dot{\gamma}(T) = 0.$$

Let us set:

$$\mathcal{M} = \begin{pmatrix} M, & -aM \\ -aM, & J_0 \end{pmatrix}, \ \mathcal{C} = \begin{pmatrix} C_{11}, & C_{12} \\ C_{21}, & C_{22} \end{pmatrix}, \ X = \begin{pmatrix} z \\ \gamma \end{pmatrix},$$
$$\mathcal{K} = \begin{pmatrix} 0, & -u^2\varrho_e R_1 \\ 0, & -u^2\varrho_e R_2 \end{pmatrix}, \ \mathcal{B} = \begin{pmatrix} \varrho_e u^2 G_1 \\ \varrho_e u^2 G_2 \end{pmatrix}, \ \mathcal{E} = \begin{pmatrix} \varrho_e u E_1 \\ \varrho_e u E_2 \end{pmatrix},$$

where we have introduced the notations:

$$\begin{aligned} &G_1 = \tfrac{S_f}{2}\frac{\partial c_{zf}}{\partial\gamma}(\alpha_0), \ \ G_2 = \frac{S_f}{2}\big[L\frac{\partial c_{mf}}{\partial\gamma}(\alpha_0) + d_f(\sin(\alpha_0)\frac{\partial c_{zf}}{\partial\gamma}(\alpha_0)\big], \\ &E_1 = \frac{S_f}{2}\big[2d_f c_{zf}(\alpha_0) - d_f\sin(\alpha_0)\frac{\partial c_{zf}}{\partial\gamma}(\alpha_0)\big], \\ &E_2 = \frac{S_f d_f}{2}\big[d_f(\sin(2\alpha_0)c_{zf}(\alpha_0) - \sin(\alpha_0)^2\frac{\partial c_{zf}}{\partial\gamma}(\alpha_0)) \\ &\qquad\qquad -L(\sin(\alpha_0)\tfrac{\partial c_{mf}}{\partial\gamma}(\alpha_0) + 2\cos(\alpha_0)c_{mf}(\alpha_0))\big]. \end{aligned} \tag{14}$$

This criterion for the control problem, is defined as follows for each value of the positive parameter ε representing the unitary cost of the control, by (a_0, b_0, ε are positive numbers):

$$\begin{aligned} &J^\varepsilon(\delta) = \frac{1}{2}\{|z(T)-z_0|^2 + |\dot z(T)|^2 + |\gamma(T)|^2 + |\dot\gamma(T)|^2 + \varepsilon\int_0^T [a_0\delta^2(s) + b_0\dot\delta^2(s)]ds, \\ &\mathcal{M}\ddot X - \mathcal{C}\dot X + \mathcal{K}X = \mathcal{B}\delta + \mathcal{E}\dot\delta, \ \ X(0) = X_0, \ \ \dot X(0) = X_1. \end{aligned} \tag{15}$$

The optimal control is finally defined as the solution of the following problem:

$$\min_{\delta\in H_0^1(]0,T[)} J^\varepsilon(\delta). \tag{16}$$

The first point is to formulate the optimality relation which is obtained in this case by writing that the derivative of the criterion J^ε with respect to δ is zero. This is quite classical to introduce the adjoint state P solution of the following differential system:

$$\begin{cases} \mathcal{M}\ddot P + {}^t\mathcal{C}\dot P + {}^t\mathcal{K}P = 0, \\ \mathcal{M}P(T) = \begin{pmatrix} \dot z(T) \\ \dot\gamma(T) \end{pmatrix}, \ \ \mathcal{M}\dot P(T) = -\begin{pmatrix} z(T) - z_0 \\ \gamma(T) \end{pmatrix} - {}^t\mathcal{C}P(T). \end{cases} \tag{17}$$

and the optimality relation can be written (see [9],[1]):

$$\begin{cases} \forall t \in]0,T[, \ \ {}^t\mathcal{B}P - {}^t\mathcal{E}\dot P + \varepsilon[a_0\delta - b_0\ddot\delta] = 0, \\ \delta(0) = \delta(T) = 0. \end{cases} \tag{18}$$

Remark 1. The choice of the space $H_0^1(]0,T[)$ has been done in order to have a finite cost for the control δ. The boundary conditions could be different (at $t = 0$ and $t = T$).

For instance, with free edge conditions, one would obtain more degrees of freedom for the control. But the discontinuity at the extremities, is not always a good strategy in the practical implementation. Nevertheless, this could be useful in particular case where the controllability condition is not satisfied. This point is discussed in the following.

□

The solution method can be based on a gradient or more precisely a conjugate gradient method using the gradient of J^ε which is ${}^t\mathcal{B}P+\varepsilon\delta$. But another much more efficient method recently developed, leads to a so-called phase control. Let us explain how to characterize the corresponding control law.

Let us set *a priori*:

$$\begin{cases} X = X^0 + \varepsilon X^1 + \dots, \\ P = P^0 + \varepsilon P^1 + \dots, \\ \delta = \delta^0 + \varepsilon\delta^1 + \dots \end{cases} \tag{19}$$

By introducing *a priori* these expression into the system (15)-(17)-(18) and bu equatting the terms of same power in the resulting expressions, one obtains:

- **Order 0**

$$\begin{cases} \mathcal{M}\ddot{X}^0 - \mathcal{C}\dot{X}^0 + \mathcal{K}X^0 = \mathcal{B}\delta^0 + \mathcal{E}\dot{\delta}^0,\ X^0(0) = X_0,\ \dot{X}^0(0) = X_1, \\ \mathcal{M}\ddot{P}^0 + {}^t\mathcal{C}\dot{P}^0 + {}^t\mathcal{K}P^0 = 0, \\ \mathcal{M}P^0(T) = \dot{X}(T),\ \mathcal{M}\dot{P}^0(T) = -\begin{pmatrix} z^0(T) - z_0 \\ \gamma^0(T) \end{pmatrix} - {}^t\mathcal{C}P^0(T), \\ \forall t \in]0,T[,\ {}^t\mathcal{B}P^0 - {}^t\mathcal{E}\dot{P}^0 = 0, \end{cases} \tag{20}$$

- **Order 1**

$$\begin{cases} \mathcal{M}\ddot{X}^1 - \mathcal{C}\dot{X}^1 + \mathcal{K}X^1 = \mathcal{B}\delta^1 + \mathcal{E}\dot{\delta}^1,\ X^1(0) = 0,\ \dot{X}^1(0) = 0, \\ \mathcal{M}\ddot{P}^1 + {}^t\mathcal{C}\dot{P}^1 + {}^t\mathcal{K}P^1 = 0, \\ \mathcal{M}P^1(T) = \dot{X}^1(T),\ \mathcal{M}\dot{P}^1(T) = -\begin{pmatrix} z^1(T) \\ \gamma^1(T) \end{pmatrix} - {}^t\mathcal{C}P^1(T), \\ [a_0\delta^0 - b_0\ddot{\delta}^0] + {}^t\mathcal{B}P^1 - {}^t\mathcal{E}\dot{P}^1 = 0. \end{cases} \tag{21}$$

- ...

Our first point is to prove that with reasonable assumptions, one has $P^0 = 0$. This is in fact an exact controllability result for $z^0(T),\ \dot{z}^0(T), \dot{\gamma}^0(T)$ and $\gamma^0(T)$ as it will appear in the following because it will imply that $z^0(T) = z_0,\ \dot{z}^0(T) = \dot{\gamma}^0(T) = \gamma^0(T) = 0$. Let us now turn to a controllability result wich is a more adapted version of the general Bellman's result [**?**].

Theorem 6.1. *Let us assume that the vectors $\mathcal{B}$, $\mathcal{E}$ are linearly independent. Let us introduce the dual basis $\mathcal{B}^*$, $\mathcal{E}^*$ defined by ($(.,.)_2$ is the scalar product in $\mathbb{R}^2$):*

$$(\mathcal{B}^*, \mathcal{B})_2 = 1,\ (\mathcal{B}^*, \mathcal{E})_2 = 0,\ (\mathcal{E}^*, \mathcal{E})_2 = 1,\ (\mathcal{E}^*, \mathcal{B})_2 = 0.$$

We set:

$$\begin{cases} H = \mathcal{M}^{-1}\,{}^t\mathcal{C},\ L = \mathcal{M}^{-1}\,{}^t\mathcal{K}, \\ \\ Z_1 = H\mathcal{B}^*,\ Z_2 = H\mathcal{E}^*,\ Z_3 = L\mathcal{B}^*,\ Z_4 = L\mathcal{E}^*. \end{cases}$$

First of all it is assumed that:

$$(Z_4, \mathcal{E})_2 \neq 0.$$

Let r_i be the two roots of the following second degree equation:

$$r^2(Z_4,\mathcal{E})_2 + r\big[(Z_4,\mathcal{E})_2(Z_1,\mathcal{B})_2 - (Z_4,\mathcal{B})_2(Z_1,\mathcal{E})_2\big]$$
$$+\big[(Z_4,\mathcal{E})_2(Z_2,\mathcal{B})_2 - (Z_4,\mathcal{B})_2(Z_2,\mathcal{E})_2 + (Z_4,\mathcal{E})_2(Z_3,\mathcal{B})_2 - (Z_4,\mathcal{B})_2(Z_3,\mathcal{E})_2\big].$$

Then, if the roots are such that:

1. *If $r_1 \neq r_2$ (single roots), and if none theses roots is solution of:*

$$i = 1, 2 :\ r_i^2\big[1 + (Z_1,\mathcal{E}_2)\big] + r_i\big[(Z_2,\mathcal{E})_2 + (Z_3,\mathcal{E})_2\big] + (Z_4,\mathcal{E})_2 = 0.$$

2. *If $r_1 = r_2$ (double roots) in addition to the previous condition, r_1 should be such that:*

$$r_1^2\big[1 + (Z_1,\mathcal{E})_2\big] - (Z_4,\mathcal{E})_2 \neq 0,$$

the solution P^0 is zero.

As a consequence, from the final conditions satisfied by $P^0(T)$ and $\dot{P}^0(T)$ this implies that necessarily one has:

$$z(T) = z_0,\ \dot{z}(T) = \dot{\gamma}(T) = \gamma(T) = 0.$$

Proof

The vector P^0 can be explicited in the dual basis $(\mathcal{B}^*, \mathcal{E}^*)$ by:

$$P^0(t) = \xi_1(t)\mathcal{B}^* + \xi_2(t)\mathcal{E}^*.$$

Therefore:

$$\begin{cases} \ddot{\xi}_1 + \dot{\xi}_1(Z_1,\mathcal{B})_2 + \dot{\xi}_2(Z_2,\mathcal{B})_2 + \xi_1(Z_3,\mathcal{B})_2 + \xi_2(Z_4,\mathcal{B})_2 = 0, \\ \\ \ddot{\xi}_2 + \dot{\xi}_1(Z_1,\mathcal{E})_2 + \dot{\xi}_2(Z_2,\mathcal{E})_2 + \xi_1(Z_3,\mathcal{E})_2 + \xi_2(Z_4,\mathcal{E}) = 0, \\ \\ \xi_1 = \dot{\xi}_2. \end{cases}$$

This implies that:

$$\begin{cases} \ddot{\xi}_1 + \dot{\xi}_1(Z_1,\mathcal{B})_2 + \xi_1[(Z_2,\mathcal{B})_2 + (Z_3,\mathcal{B})_2] + \xi_2(Z_4,\mathcal{B})_2 = 0, \\ \\ \dot{\xi}_1[1 + (Z_1,\mathcal{E})_2] + \xi_1[(Z_2,\mathcal{E})_2 + (Z_3,\mathcal{E})_2] + \xi_2(Z_4,\mathcal{E}) = 0, \\ \\ \xi_1 = \dot{\xi}_2. \end{cases}$$

Or else:

$$\begin{cases} \ddot{\xi}_1(Z_4,\mathcal{E})_2 + \dot{\xi}_1\big[(Z_4,\mathcal{E})_2(Z_1,\mathcal{B})_2 - (Z_4,\mathcal{B})_2(Z_1,\mathcal{E})_2\big] \\ +\xi_1\big[(Z_4,\mathcal{E})_2((Z_2,\mathcal{B})_2 + (Z_3,\mathcal{B})_2) - (Z_4,\mathcal{B})_2((Z_2,\mathcal{E})_2 + (Z_3,\mathcal{E})_2)\big] = 0, \\ \dot{\xi}_1[1 + (Z_1,\mathcal{E})_2] + \xi_1[(Z_2,\mathcal{E})_2 + (Z_3,\mathcal{E})_2] + \xi_2(Z_4,\mathcal{E})_2 = 0, \\ \xi_1 = \dot{\xi}_2. \end{cases} \tag{22}$$

The solutions of the first above equation are $\xi_1(t) = A_i e^{r_i t}$ where r_i is a root of the caracteristic equation:

$$r^2(Z_4,\mathcal{E})_2 + r\big[(Z_4,\mathcal{E})_2(Z_1,\mathcal{B})_2 - (Z_4,\mathcal{B})_2(Z_1,\mathcal{E})_2\big]$$
$$+\big[(Z_4,\mathcal{E})_2(Z_2,\mathcal{B})_2 - (Z_4,\mathcal{B})_2(Z_2,\mathcal{E})_2 + (Z_4,\mathcal{E})_2(Z_3,\mathcal{B})_2 - (Z_4,\mathcal{B})_2(Z_3,\mathcal{E})_2\big].$$

Hence, assuming in a first step that the roots are single: $\xi_2(t) = \dfrac{A_i}{r_i} e^{r_i t} + c_0$ (constant).

Introducing this result into the second equation (22), one obtains for each of the three sets of solutions: $i = 1,2:\ (e^{r_i t}, \dfrac{e^{r_i t}}{r_i}),\ (0, c_0)$ the necessary relations:

$$\begin{cases} i = 1,2:\ r_i^2\big[1 + (Z_1,\mathcal{E}_2)\big] + r_i\big[(Z_2,\mathcal{E})_2 + (Z_3,\mathcal{E})_2\big] + (Z_4,\mathcal{E})_2 = 0, \\ \text{and:} \\ (Z_4,\mathcal{E})_2 = 0. \end{cases} \tag{23}$$

Finally, if none of these three relations is satisfied it implies that:

$$\forall t \in [0,T]:\ \xi_1(t) = \xi_2(t) = 0 => \forall t \in [0,T]:\ P^0(t) = 0.$$

The theorem is proved. Let us discuss now what happens if the rootsof (22) are double: $r_1 = r_2$. The solutions of (22) are now:

$$\xi_1(t) = Ae^{r_1 t}, \xi_2(t) = \frac{A}{r_1} e^{r_1 t} \text{ and } \xi_1(t) = Bte^{r_1 t},\ \xi_2(t) = B(rt-1)\frac{e^{rt}}{r^2}. \tag{24}$$

Hence the additional controllability condition is (one is the same as before):

$$r_1^2\big[1 + (Z_1,\mathcal{E})_2\big] - (Z_4,\mathcal{E})_2 \neq 0. \tag{25}$$

□

Remark 2. The controllability condition given in theorem 6.1 can be discussed in particular cases. For instance let us imagine that the damping matrix $\mathcal{C}$ is neglected (therefore $\mathcal{E} = 0$), and we choose $b_0 = 0$ (hence $\delta \in L^2(]0,T[)$. We loose the possibility to prescribe the boundary conditions on δ. Let us introduce a vector $\mathcal{E}$ orthogonal to $\mathcal{B}$ and such that $(\mathcal{E},\mathcal{E})_2 = 1$. The last relation (20) implies that:

$$P^0(t) = \xi(t)\mathcal{E}.$$

But the equation satisfied by P^0 leads to:

$$\begin{cases} \xi\ (\mathcal{M}^{-1}\ {}^t\mathcal{K}\mathcal{E},\mathcal{B})_2 = 0, \\ \ddot{\xi} + \xi\ (\mathcal{M}^{-1}\ {}^t\mathcal{K}\mathcal{E},\mathcal{E})_2 = 0, \end{cases}$$

and therefore if:

$$(\mathcal{M}^{-1}\ {}^t\mathcal{K}\mathcal{E}, \mathcal{B})_2 \neq 0$$

one can claim that the system can be exactly controlled by a function δ^0 that we will define in the following. This condition is simplier than the one with a damping, but it is less realistic as far as the velocities are such that the damping is not negligible.

□

Remark 3. If there was no rudder, the matrix $\mathcal{K}$ which has only the second row different from zero, is reduced to the vector $\mathcal{B}$. Hence one has ${}^t\mathcal{K}\mathcal{E}^* = 0$. Or else $Z_4 = 0$. One can check easily that the controllability requirements are not satisfied in such a case and this is not surprising.

□

6.2. **Characterization of the exact control δ^0.** In order to define $\delta^0 \in H_0^1(]0,T[)$ we make use of the system of order one in ε. We know from this system of relations, that :

$$a_0\delta^0 - b_0\ddot{\delta}^0 = -{}^t\mathcal{B}P^1 + {}^t\mathcal{E}\dot{P}^1, \quad \delta^0(0) = \delta^0(T) = 0,$$

but P^1 is still unknown and the next step is to compute it.
Let us introduce a vector Q depending on the time variable, and such that:

$$\mathcal{M}\ddot{Q} + {}^t\mathcal{C}\dot{Q} + {}^t\mathcal{K}Q = 0, \ \ Q(0) = \delta\Phi_1, \ \ \dot{Q}(0) = \Phi_2. \tag{26}$$

By multiplying the equation of order zero by Q and by integrating from 0 to T, one obtains (taking into account that $X^0(T) = \dot{X}(T) = 0$):

$$\begin{cases} \displaystyle\int_0^T (\mathcal{M}\ddot{X}^0, Q)_2 - \int_0^T (\mathcal{C}\dot{X}^0, Q)_2 + \int_0^T (\mathcal{K}X^0, Q)_2 \\ \displaystyle = -(\mathcal{M}\dot{X}^0(0), Q(0))_2 + (\mathcal{M}X^0(0), \dot{Q}(0))_2 + (CX^0(0), Q(0))_2 \\ \displaystyle = \int_0^T [(\mathcal{B}, Q)_2 - (\mathcal{E}, \dot{Q})_2]\delta^0. \end{cases}$$

The control δ^0 can be obtained in different ways. One consists in using Fourier series and this leads to:

$$\begin{cases} \delta^0(t) = \dfrac{2}{T}\displaystyle\sum_{n\geq 0} A_n \sin(\frac{n\pi t}{T}), \\ \\ \text{with:} \\ \\ A_n = -\dfrac{\displaystyle\int_0^T [(\mathcal{B}, P^1)_2(s) - (\mathcal{E}, \dot{P}^1)_2(s)]\sin(\frac{n\pi s}{T})ds}{a_0 + b_0\frac{n^2\pi^2}{T^2}}. \end{cases} \tag{27}$$

But δ^0 can also be computed from (20) as follows in order to avoid the difficulties connected with the Gibbs phenomenon in the Fourier series:

$$\delta^0(t) = A_0\cosh(rt) + B_0\sinh(rt) + \int_0^t f(s)\sinh(r(t-s))ds,$$

with:

$$r = \sqrt{\frac{a_0}{b_0}},\quad B_0 = -\frac{\displaystyle\int_0^T f(s)\sinh(r(t-s))ds}{\sinh(rT)},\quad A_0 = 0, \tag{28}$$

$$f(s) = \frac{(\mathcal{B}, P^1(s))_2 - (\mathcal{E}, \dot{P}^1(s))_2}{b_0 r}.$$

Let us set, choosing for instance, the expression given by the Fourier series:

$$\begin{cases} \Phi = (P^1(0), \dot{P}^1(0)),\ \delta\Phi = (Q(0), \dot{Q}(0)), \\ \\ G_1(s) = (\mathcal{B}, Q^1)_2(s) - (\mathcal{E}, \dot{Q}^1)_2(s), \quad B_n = -\displaystyle\int_0^T G_1(s)\sin(\frac{n\pi s}{T})ds, \\ \\ \Lambda(\Phi, \delta\Phi) = \dfrac{2}{T}\displaystyle\sum_{n\geq 0} A_n B_n, \\ \\ L(\delta\Phi) = (\mathcal{M}\dot{X}^0(0), Q(0))_2 - (\mathcal{M}X^0(0), \dot{Q}(0))_2 - (CX^0(0), Q(0))_2, \end{cases} \tag{29}$$

and the problem to be solved in order to characterize Φ and therefore the exact control δ^0; consists in finding the solution of:

$$\Phi \in \mathbb{R}^2 \times \mathbb{R}^2,\ \forall \delta\Phi \in \mathbb{R}^2 \times \mathbb{R}^2,\ \Lambda(\Phi, \delta\Phi) = L(\delta\Phi). \tag{30}$$

Remark 4. The expression of $\Lambda(.,.)$ can also be obtained using the other expression of δ^0 given at (28) with more accuracy from the numerical point of view.

Let us now check the solvency of (30). The bilinear form Λ is clearly symmetrical and positive. The continuity is also straightforward. The same is true for the linear form L. Furthermore if $\Phi \in \mathbb{R}^4$ is such that: $\Lambda(\Phi, \Phi) = 0$ one has (Φ being associated to P^1 in the next expression):

$$\forall n \in \mathbb{N}, \int_0^T [(\mathcal{B}, P^1)_2(s) - (\mathcal{E}, \dot{P}^1)_2(s)]\sin(\frac{n\pi s}{T})ds = 0,$$

which implies that the control δ linked to P^1, is solution of the variational model, which has a unique solution:

$$\begin{cases} \text{find } \delta \in H_0^1(]0,T[) \text{ such that:} \forall v \in H_0^1(]0,T[), \\ \\ \displaystyle\int_0^T a_0\delta v + b_0\dot{\delta}\dot{v} = -\int_0^T [(\mathcal{B}, P^1)_2(s) - (\mathcal{E}, \dot{P}^1)_2(s)]v(s)ds. \end{cases} \tag{31}$$

Because this solution can be written:

$$\delta = \sum_{n\geq 0} A_n \sin(\frac{n\pi t}{T}),$$

and because $A_n = 0$ one can conclude that $\delta = 0$ and finally that the bilinear form is positively definite. Hence, the system (30) enables to define Φ uniquely. Conversely if the control δ^0 is defined at (28) where P^1 is solution of (30), the solution X of the initial system, satisfies because of (30) (X_d is the vecteur of $\mathbb{R}^2$ where only the first component is different from zero and equal to z_0):

$$(\mathcal{M}(X^0(T) - X_d), \dot{Q}(T)) = (\mathcal{M}\dot{X}^0(T) - \mathcal{C}X^0(T), \dot{Q}(T)) = 0. \tag{32}$$

where Q is solution of:

$$\begin{cases} \forall (Q_0, Q_1) \in \mathbb{R}^4, \ \ Q \text{ being solution of} \\ \\ Q(0) = (Q_0, Q_1), \ \mathcal{M}\ddot{Q} + {}^t\mathcal{C}\dot{Q} + \mathcal{K}Q = 0, \end{cases} \tag{33}$$

But $(Q(T), \dot{Q}(T))$ can reach any values in $\mathbb{R}^4$ as far as one can prescribe any value on the initial condition for Q. Therefore, this implies that:

$$z^0(T) = z_0, \ \dot{z}^0(T) = \gamma^0(T) = \dot{\gamma}^0(T) = 0. \tag{34}$$

This proves that the control δ^0 is exact. Let us summarize the obtained results in the following statement.

Theorem 6.2. *Let us assume the hypothesis of theorem 6.1. The bilinear form $\Lambda(.,.)$ defined on $\mathbb{R}^2 \times \mathbb{R}^2$ at equation (29) is associated to a symmetrical and positively definite matrix with dimension 4×4 -say $\mathcal{G}$. The linear form L is associated to a vector of $\mathbb{R}^4$ denoted by $\mathcal{L}$. The following linear equation has a unique solution:*

$$\mathcal{G}\Phi = \mathcal{L},$$

and if P^1 is the solution of:

$$\mathcal{M}\ddot{P}^1 + {}^t\mathcal{C}\dot{P}^1 + {}^t\mathcal{K}P^1 = 0, \ (P^1(0), \dot{P}^1(0)) = \Phi.$$

With this set of initial conditions, the function δ^0 given (for instance), at (31) is an exact control, depending on the control time T and the initial conditions $(X(0), \dot{X}(0))$. Furthermore, δ^0 is the unique exact control in the space $H_0^1(]0,T[)$ wich minimizes the norm:

$$v \in H_0^1(]0,T[) \to \sqrt{a_0 \int_0^T v^2 + b_0 \int_0^T \dot{v}^2}$$

.

Proof The only point which remains to be justified, concerns the last point of the statement of the theorem. Let us first denote by $\mathcal{U}^{ad}$ the convex set (not a vectorial space) defined by:

$$\begin{cases} \mathcal{U}^{ad} = \{v \in H_0^1(]0,T[), \ Y(T) = \dot{Y}(T) = 0\}, \\ \\ \text{where } Y \text{ is solution of the second equation (15) with the control } v. \end{cases} \tag{35}$$

Hence $\delta^0 \in \mathcal{U}^{ad}$, one can claim that $\mathcal{U}^{ad} \neq \emptyset$. Furthermore the mapping:

$$\forall v \in \mathcal{U}^{ad} \to a_0 \int_0^T v^2 + b_0 \int_0^T \dot{v}^2,$$

is strictly convex and therefore there is a unique solution -say δ^*- to the problem:

$$\min_{v \in \mathcal{U}^{ad}} \frac{1}{2}[a_0 \int_0^T v^2 + b_0 \int_0^T \dot{v}^2].$$

It is characterized by (see for instance [5]):

$$\forall v \in \mathcal{U}^{ad}, a_0 \int_0^T \delta^*(v-\delta^*) + b_0 \int_0^T \dot{\delta}^*(\dot{v}-\dot{\delta}^*) = 0.$$

But δ^0 which is given by (28), where P^1 is solution of (30), also satisfies (because v and δ^0 are both exact control):

$$\forall v \in \mathcal{U}^{ad},\ a_0 \int_0^T \delta^0(v-\delta^0) + b_0 \int_0^T \dot{\delta}^0(\dot{v}-\dot{\delta}^0) = 0.$$

Hence, by setting $v = \delta^0$ in the first relation and $v = \delta^*$ in the second one, and adding the two obtained equalities, one gets $\delta^0 = \delta^*$. □

6.3. **A mathematical result on the convergence.** Let us introduce the gap variables by:

$$\overline{X} = X - X^0,\ \overline{P} = P - \varepsilon P^1,\ \overline{\delta} = \delta - \delta^0. \tag{36}$$

From the definition of δ and because δ^0 is an exact control law, one obtains:

$$\begin{cases} J^\varepsilon(\delta) \leq J^\varepsilon(\delta^0) = \dfrac{1}{2}[||X^0(T) - X_d||_2^2 + ||\dot{X}^0||_2^2 + \varepsilon(a_0 \displaystyle\int_0^T |\delta^0|^2 + b_0 \int_0^T |\dot{\delta}|^2)] \\ \\ = \dfrac{\varepsilon}{2}(a_0 \displaystyle\int_0^T |\delta^0|^2 + b_0 \int_0^T \dot{\delta}^2). \end{cases}$$

And therefore ($||\ .\ ||_{1,2,]0,T[}$ is the norm used in the space $H_0^1(]0,T[)$):

$$\forall \varepsilon > 0,\ \ ||\delta||_{1,2,]0,T[} \leq ||\delta^0||_{1,2,]0,T[} = \text{ constant versus } \varepsilon.$$

This enables one to deduce that there is a subsequence (with respect to ε) still denoted by δ such that (using the weak lower semi-continuity for convex functions):

$$\lim_{\varepsilon \to 0} \delta = \delta^* \in H_0^1(]0,T[) - weak \text{ and:}$$

$$a_0||\delta^*||_{0,]0,T[}^2 + b_0||\dot{\delta}^*||_{0,]0,T[}^2 \leq a_0||\delta^0||_{0,]0,T[}^2 + b_0||\dot{\delta}^0||_{0,]0,T[}^2.$$

From:

$$a_0||\delta - \delta^*||_{0,]0,T[}^2 + b_0||\dot{\delta} - \dot{\delta}^*||_{0,]0,T[}^2 =$$

$$a_0||\delta||_{0,]0,T[}^2 + b_0||\dot{\delta}||_{0,]0,T[}^2 - 2a_0 \int_0^T \delta\delta^* - 2b_0 \int_0^T \dot{\delta}\dot{\delta}^* + a_0||\delta^*||^2 + b_0||\dot{\delta}^*||_{0,]0,T[}^2$$

$$\leq 2a_0 \int_0^T \delta^*(\delta^* - \delta) + 2b_0 \int_0^T \dot{\delta}^*(\dot{\delta}^* - \dot{\delta}) \to_{\varepsilon \to 0} 0,$$

we deduce the strong convergence of δ to δ^* when $\varepsilon \to 0$ and therefore the one of the corresponding subsequence $(X(T) - X_d, \dot{X}(T))$ to $(0,0)$, because of the continuity of the state variable with respect to the control law.
In addition one has (lower semi-continuity of continuous convex functions):

$$\forall v \in H_0^1(]0,T[),\ a_0||\delta^*||_{0,]0,T[}^2 + b_0||\dot{\delta}^*||_{0,]0,T[}^2 = \lim_{\varepsilon \to 0} J^\varepsilon(\delta) \leq J^\varepsilon(v),$$

and in particular if $v \in \mathcal{U}^{ad}$, one gets:

$$a_0||\delta^*||_{0,]0,T[}^2 + b_0||\dot{\delta}^*||_{0,]0,T[}^2 \leq a_0||v||_{0,]0,T[}^2 + b_0||\dot{v}||_{0,]0,T[}^2,$$

which proves (Tychonov's result [19]) that the control δ^* minimizes the norm:

$$v \to a_0||v||^2_{0,]0,T[} + b_0||\dot{v}||^2_{0,]0,T[},$$

and therefore it is precisely the control δ^0 found by the asymptotic expansion. Hence there is only one accumulation point to the sequence δ which converges to δ^0 when $\varepsilon \to 0$. Let us summarize the obtained result in the next statement.

Theorem 6.3. *Let us assume the hypothesis of theorem 6.1. Then there exists a unique exact control for a given time control T and for any initial conditions which realizes the minimum of the norm:*

$$v \to a_0||v||^2_{0,]0,T[} + b_0||\dot{v}||^2_{0,]0,T[},$$

in the space $H^1_0(]0,T[)$ among the exact control. This control -say δ^0- is the one given in theorem 6.2.

Remark 5. The exact control depends on the data ad on the time delay T. But the smallest is T the larger will be the magnitude of the control. And because there is a limitation on the amplitude of the rake (which is the control), it is necessary to discuss the effect of a constraint on the control. This is the goal of the next section.

6.3.1. *Few numerical simulation.* We have plotted the evolution of the heaving, the pitching and the exact control law on the figure 10, 11 and 13 versus the time and for four velocities of the boat (5 m/s, 10 m/s, 15 m/s, 20 m/s). In each case we choose $T = 10s$. But T is a variable which can be adjusted. Nevertheless the smallest is T the larger will be the magnitiude of the solution during the control process. One can observe that the control is a law frequency one. The efficiency is quite satisfying. But clearly it is not obvious to manufacture it without special tricks as far as no electronical device is allowed.

6.4. **Control with constraints.** In practice the magnitude of the control is restricted. Therefore the minimisation of the criterion J^ε should be performed over the bounded set:

$$K = \{q \in H^1_0(]0,T[), \text{ such that: } |q| \leq q_{max}\}. \tag{37}$$

The new control problem is now:

$$\min_{\delta \in K} J^\varepsilon(\delta). \tag{38}$$

From classical results in optimisation, the optimal solution is characterized by:

$$\begin{cases} \delta \in K, \\ \\ ae\ t\ \in]0,T[,\ \ \forall q \in K,\ G^\varepsilon(\delta)(q-\delta) \geq 0, \end{cases} \tag{39}$$

or else, by expliciting the gradient of J^ε:

$$\begin{cases} ae\ t \in]0,T[,\ \forall q \in K,\ (\varepsilon[a_0\delta - b_0\ddot{\delta}] + {}^t\mathcal{B}P - {}^t\mathcal{E}P)(q-\delta) \geq 0, \\ \\ \forall q \in \mathbb{R},\ \ |q| \leq q_{max},\ \dot{\delta}(T)(q-\delta(T)) \geq 0,\ \dot{\delta}(T)(q-\delta(T)) \leq 0. \end{cases} \tag{40}$$

For $\varepsilon \to 0$ one can define a limit control problem (see [20]) following the same idea as in the previous section, but with a different strategy. Let us consider two following possibilities.

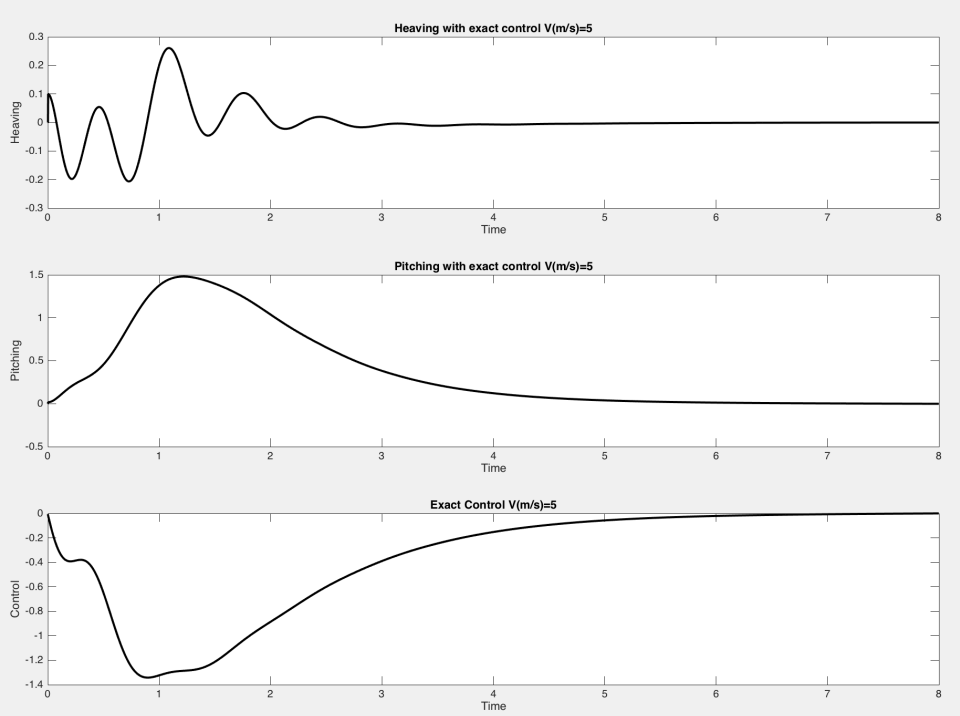

FIGURE 10. u=5m/s

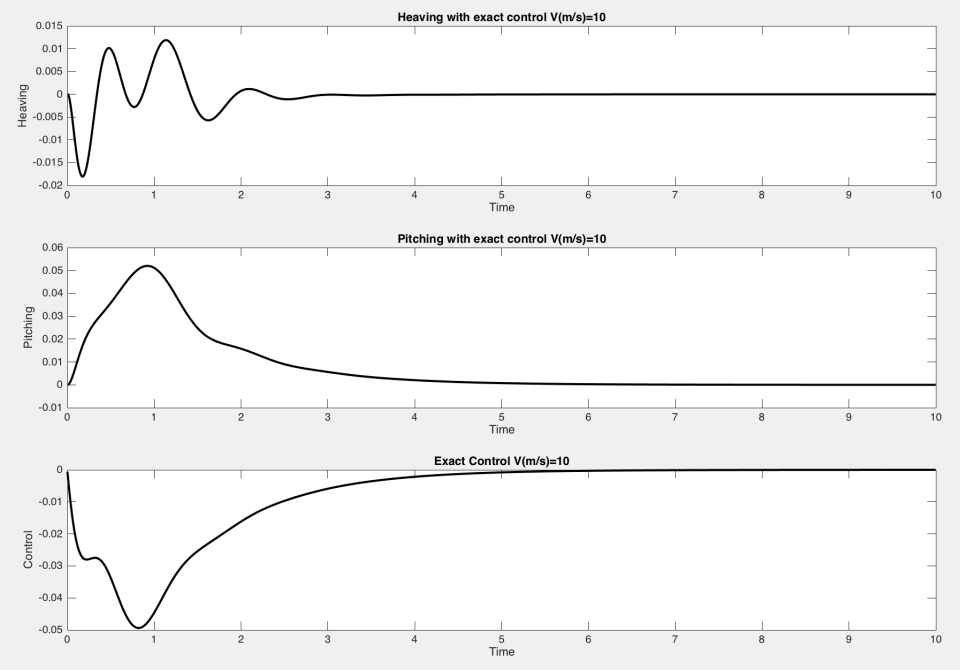

FIGURE 11. u=10m/s

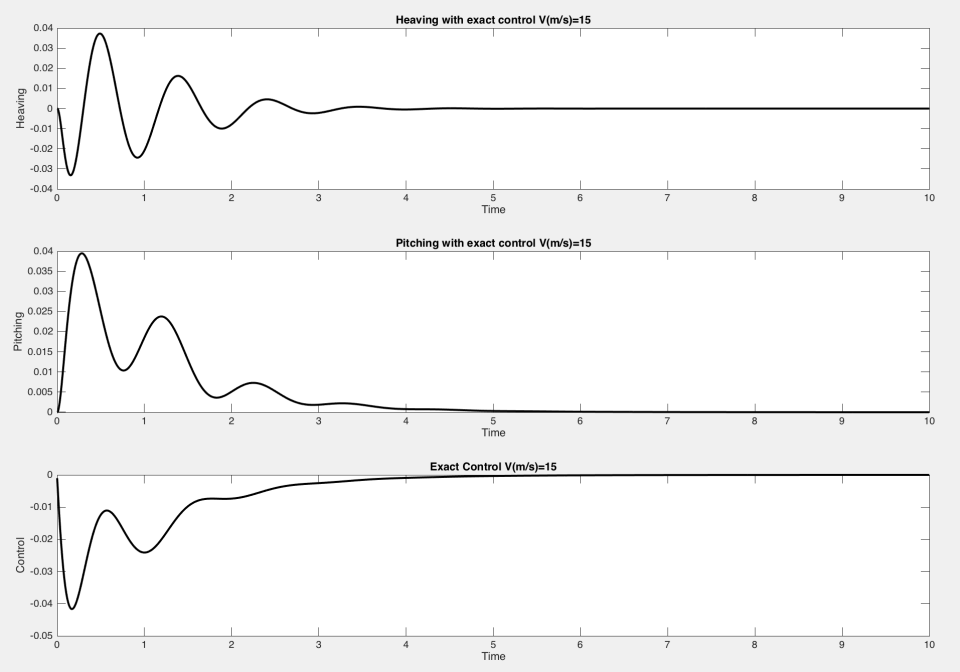

FIGURE 12. u=15m/s

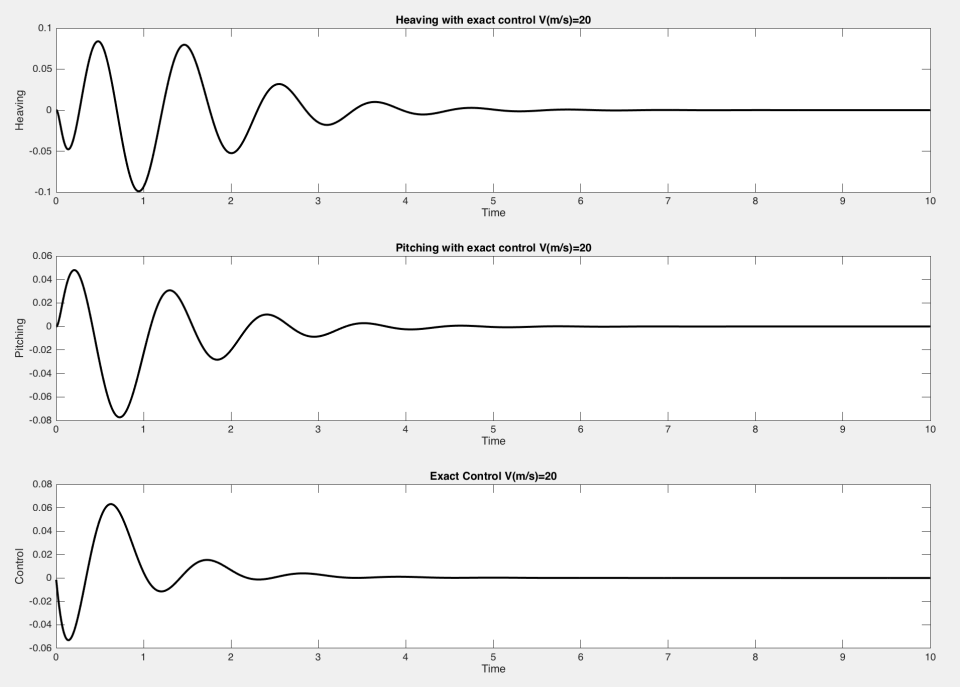

FIGURE 13. u=20m/s

6.4.1. *Assuming that there is an exact control -say $\delta^0 \in K$ for the initial conditions and the time control T.* In this case one has ($\delta \in K$ is the unique solution of (38) and is such that:

$$\delta \in K, \ \ \forall v \in K, \ J^\varepsilon(\delta) \leq J^\varepsilon(v),$$

and by choosing $v = \delta^0$:

$$\begin{cases} a_0||\delta||^2_{0,]0,T[} + b_0||\dot{\delta}||^2_{0,]0,T[} \leq a_0||\delta^0||^2_{0,]0,T[} + b_0||\dot{\delta}^0||^2_{0,]0,T[} \\ \\ \text{and} \\ \\ ||X(T) - X_d||_2^2 + ||\dot{X}(T)||_2^2 \leq C\varepsilon. \end{cases}$$

Hence, δ is bounded in the space $H^1(]0,T[)$ and one can extract a subsequence (with respect to ε but we keep the notation ε because there is no ambiguïty) such that:

$$\lim_{\varepsilon \to 0} \delta = \delta^* \ \text{ in the space } H_0^1(]0,T[) - weak.$$

Furthermore one can ensure that:

$$\lim_{\varepsilon \to 0} ||X(T) - X_d||_2^2 + ||\dot{X}(T)||_2^2 = 0.$$

But X as function of the space $[\mathcal{C}^2([0,T])]^2$ depends continuously of δ as a function of $H^1(]0,T[)$. Hence X tends to X^* solution obtained with the control δ^* and therefore satisfies: $X^*(T) = 0, \ \dot{X}^*(T) = 0$. Hence δ^* is an exact control with the minimum norm used on $H^1(]0,T[)$. Because it is unique (the norm is strictly convex) all the sequence δ converges weakly in $H^1(]0,T[)$ to δ^*. The adjoint state P tends also in the space $[\mathcal{C}^1([0,T])]^2$ to zero because it depends continuously on the final condition. And therefore $\lim_{\varepsilon \to 0} P = 0$ in $\mathcal{C}^1([0,T])$-strongly (and even more). One can also prove easily (as previously) that the convergence of the control δ to δ^0 is strong in the space $H_0^1(]0,T[)$.

6.4.2. *Assuming that there is no exact control in K for the initial conditions and the time control T.* The control $\delta \in K$ is still bounded in $L^2(]0,T[)$ and there is a subsequence still denoted by δ such that $\lim_{\varepsilon \to 0} \delta = \delta^*$ in $L^2(]0,T[) - weak$. Following the justification given above, one can also claim that the corresponding subsequence of P tends to P^* in $[\mathcal{C}^1([0,T])]^2$. And $P^* \neq 0$ or else one would have $X^*(T) - X_d = \dot{X}^*(T) = 0$, which is excluded by hypothesis or else one would have $\delta^* \in K$ and it would be an exact control. From (40) one can state that:

$$\forall q \in K, \ \int_0^T {}^t\mathcal{B}P^*(q - \delta^*) \geq 0.$$

Or else:

$$ae \ t \in]0,T[, \ \delta^*(t) = -q_{max}\text{sign}({}^t\mathcal{B}P^*)(t).$$

It means that the control δ^* is *bang-bang* (ie. takes the extremum values for almost all $t \in]0,T[$). Therefore the L^2 norm of δ^* is equal to $\sqrt{T}q_{max}$. But we can't guaranty the uniqueness. Therefore it is worth to choose T in order to ensure that there exists an exact control, otherwise some instabilities could appear in the computation of δ (with $\varepsilon > 0$), even if it is unique (and in the space $H_0^1(]0,T[)$) but for any ε small enough.

Remark 6. Usually the R. Bellman condition [1] and the fact that the real part of the eigenvalues of the characteristic equation of the linear system, are negative are sufficient conditions to ensure that there exists an exact control but with a control time which can be larger than the one used in the computation of the exact control without constraint. The minimum time T_{min} for an exact control is the boundary between the existence and the non-existence of an exact control in the set K. Neverthelesse the bang-bang control should be avoided in this case (as for an aircraft) because it is not robust and implies shocks which can be at the origin of unwanted perturbations. Therefore, knowing the maximum amplitude q_{max} of the control, it is possible to compute the minimum control time -say T_{min}- and therefore to ensure that the exact control law is computed with a control time T sufficiently larger than T_{min}.

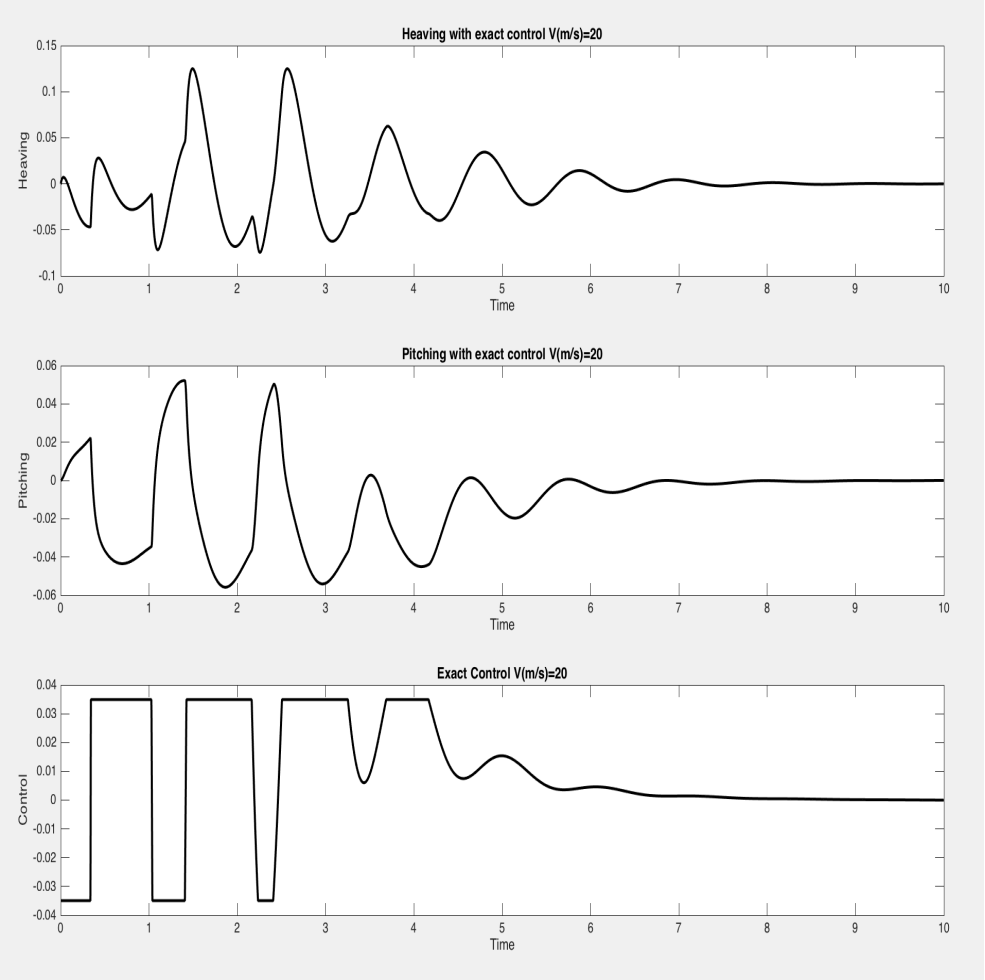

FIGURE 14. Exact control with upper bound on the magnitude of the control. The projection on the admissible set for the control is performed using the cut off method. One has on this figure V=20 m/s and the initial perturbation is large.

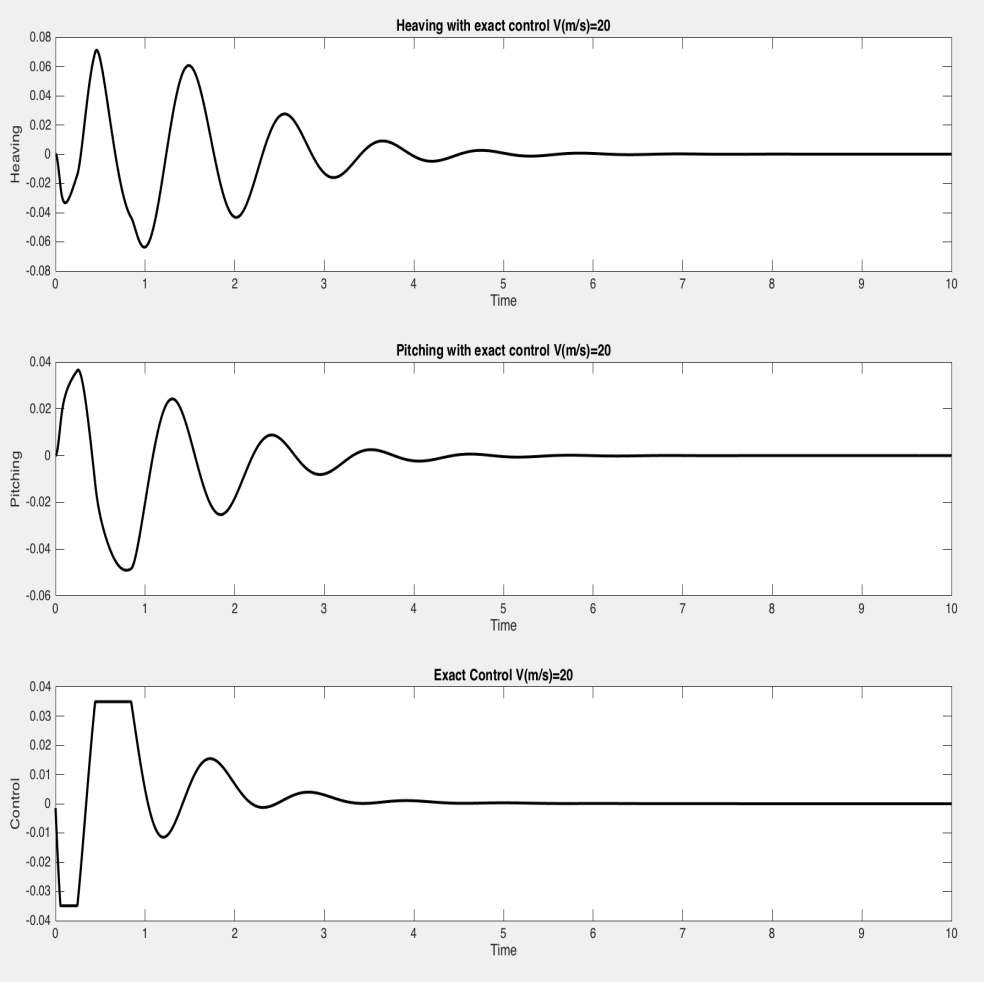

FIGURE 15. Exact control with upper bound on the magnitude of the control. There is no oscillation at the end. The maximum magnitude of the control can be adjusted but one can also modify the coefficients a_0 and b_0 and also add a transient term in the control criterion. Here one has V=20 m/s and the initial perturbation is smaller than the one on the previous figure.

6.5. **A simple proportional feed-back system.** As we have pointed out in the previous section, it is necessary to introduce the term $\dot{\delta}$ in the control law. A control which only include δ would be unstable because of the vanishing stiffness in the direction of the heaving movement. Furthermore the absolute referential for $\delta = \alpha - \alpha_0$ is not obvious in the practical implementation. But the pitching velocity is easier to detect as far as a flexible rotation is allowed at the jonction between the foil and the bow of the boat. In fact this is shown on figure 22. The flexibility can be stiffened using a spring and damped by an hydraulic ram. This is a simple feed-back loop based on prescribing the rake through this ram. Let us try to explain why this method, even if it is not optimal, is a good one for the stabilisation of the oversea flight.

In this case the flexibility of the foil is ensured around a rotational axis fixed on the bow of the ship or simply the daggerboard case. Therefore a new degree of freedom representing the rotation around this axis is introduced. Furthermore, two additional mechanical devices are introduced: one is a damper and the other is a spring. The damping coefficient is ξ and the stiffness c_f. Due to this new degree of freedom the equations of the model are a little bit changed. We introduce three new coefficients: one is the mass of the foil -say m_f- the second one is the inertia of the foil (alone) around point o -say J_f and the last one is the distance between the point o and the center of mass of the foil (alone) -say d_{og}-; they are represented on figure 16. The equations of the movement are now (we use the same

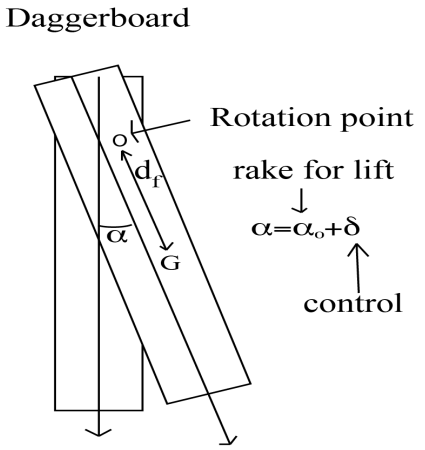

FIGURE 16. The notations used in this section

notations as before excepted that J_o and M are respectively the inertia and the mass of the ship around point o without the main foil):

$$\begin{cases} (M+m_f)\ddot{z} - aM\ddot{\gamma} + d_{og}\sin(\alpha_0)m_f\ddot{\alpha} - c_{11}\dot{z} - c_{12}(\dot{\gamma}+\dot{\alpha}) \\ \qquad\qquad + \dfrac{\varrho S u^2}{2} R_1(\gamma+\alpha) = 0, \\ -aM\ddot{z} + J_0\ddot{\gamma} - c_{21}\dot{z} - c_{22}(\dot{\gamma}+\dot{\alpha}) + \dfrac{\varrho S L u^2}{2} R_2(\gamma+\alpha) = 0, \\ d_{og}\sin(\alpha_0)m_f\ddot{z} + J_f\ddot{\alpha} - c_{21}\dot{z} - c_{22}\dot{\gamma} + (\xi - c_{22})\dot{\alpha} \\ \qquad\qquad + \dfrac{\varrho L S u^2}{2} R_2(\gamma+\alpha) + c_f\alpha = 0. \end{cases} \tag{41}$$

Let us introduce new notations for the different matrices:

$$\mathcal{M} = \begin{pmatrix} M+m_f & -aM & d_{og}\sin(\alpha_0)m_f \\ -aM & J_0 & 0 \\ d_{og}\sin(\alpha_0)m_f & 0 & J_f \end{pmatrix} \mathcal{C} = \begin{pmatrix} c_{11} & c_{12} & c_{12} \\ c_{21} & c_{22} & c_{22} \\ c_{21} & c_{22} & c_{22}-\xi \end{pmatrix}$$

$$\mathcal{K} = \begin{pmatrix} 0 & \frac{\varrho S u^2}{2}R_1 & \frac{\varrho S u^2}{2}R_1 \\ 0 & \frac{\varrho L S u^2}{2}R_2 & \frac{\varrho L S u^2}{2}R_2 \\ 0 & \frac{\varrho L S u^2}{2}R_2 & \frac{\varrho L S u^2}{2}R_2 + c_f \end{pmatrix} \qquad X = \begin{pmatrix} z \\ \gamma \\ \alpha \end{pmatrix}. \tag{42}$$

The equation (42) can therefore be written as follows (with initial conditions):

$$\mathcal{M}\ddot{X} - \mathcal{C}\dot{X} + \mathcal{K}X = 0.$$

The strong stability of the system is obtained as far as the imaginary part of the solution to the following eigenvalue problem are positive:

$$\det|-\lambda^2\mathcal{M} - i\lambda\mathcal{C} + \mathcal{K}| = 0 \tag{43}$$

In fact the larger is the least imaginary part of the solution to (43), the best is the stabilisation of the system. The evolution of the imaginary part of these solutions are plotted on figure **??** with respect to ξ for various values of c_f but with $\mathcal{C} = 0$. One can observe that the added spring c_f is not necessary for obtaining a stabilisation. In the report published by the American team for America's cup, they mention that this spring was not used (see figure 7).

6.6. **The system used by Oracle Team USA.** Let us consider the simple equation, just for explaining the strategy used, but clearly it has to be adjusted at purpose in pratice:

$$J_f\ddot{\alpha} + c_f\alpha = -\alpha_{max}\text{sign}(\dot{\alpha}),\ \alpha(0) = \alpha_0,\ \ \dot{\alpha}(0) = \alpha_1. \tag{44}$$

This is a very classical control strategy which is often used for stabilizing aircraft. It is not an exact control and the result depends on the value of the maximum amplitude α_{max}. But this can be adjusted easily by a computer on an aircraft and in the case of the America's cup boat, it requires a simple education if the helmsman. One can see on figure 18 how works the so-called input button which drive α_{max} by step of $\pm.5^0$ for each press on the control button. The rest is purely automatic and based on simple mechanical devices. The sign function is detected by the rocker switch (see figure 22).

The solution have been plotted on figure 17 for height values of α_{max}. One can see that this is stabilized system. The time delay required for the stabilisation depends on both the initial data and the maximum magnitude α_{max} of the control.

One could imagine that instead of the control $-\alpha_{max}\text{sign}(\dot{\alpha})$ one set $-\alpha_{max}\text{sign}(\alpha)$. The results are on figure 17 and show that this doesn't work at all as it is well know in any course in control theory.

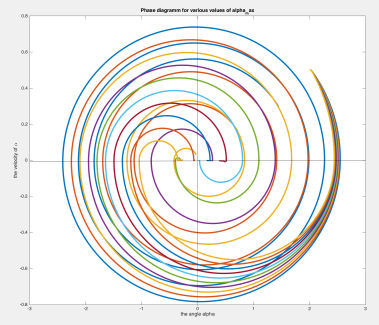

FIGURE 17. Several trajectories for different values of α_{max} starting from the same initial condition. One can observe that α_{max} should be adjusted in order to obain the right control. This is why the helmsman has a control box which enables him to adjust α_{max} by steps of $\pm.5^0$

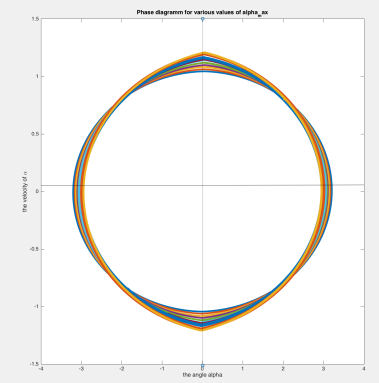

FIGURE 18. Several trajectories for different values of α_{max} starting from the same initial condition. One can observe that this control is unuseful. This is why the rocker switcher has to detect the sign of the velocity of the rake and not the one of the angle (the pitching angle).

6.7. **Comparison between the exact control, OTUSA control and exact control with upper bound.** for the same boat and foil-rudder set, we compare the obtained results. The results are given on the figures 19, 20 and 21. one can see that the OTUSA system is very efficient at the beginning but the exact control is more precise for small perturbation. The ideal solution is to couple OTUSA control law at the beginning and the exact control when the magnitude of the oscillation are small enough. In this case the mechanical manufacturing of the system can be done using a steering box with an additionnal button compared to the one of OTUSA. But this is another study not included in this analysis. The use of a system of mass, sring and dashpot can lead to a suitable approximation of the exact feedback. Because the matrix leading to the exact control with respect to the perturbation is only dependent on the ship. It is in this study a 4×4 symmetrical matrix which therefore depends on only 10 coefficients. A least square method can be applied in order to give a fine approximation of this impedance using a proportional-integral-derivative composed of several mechanical blocks.

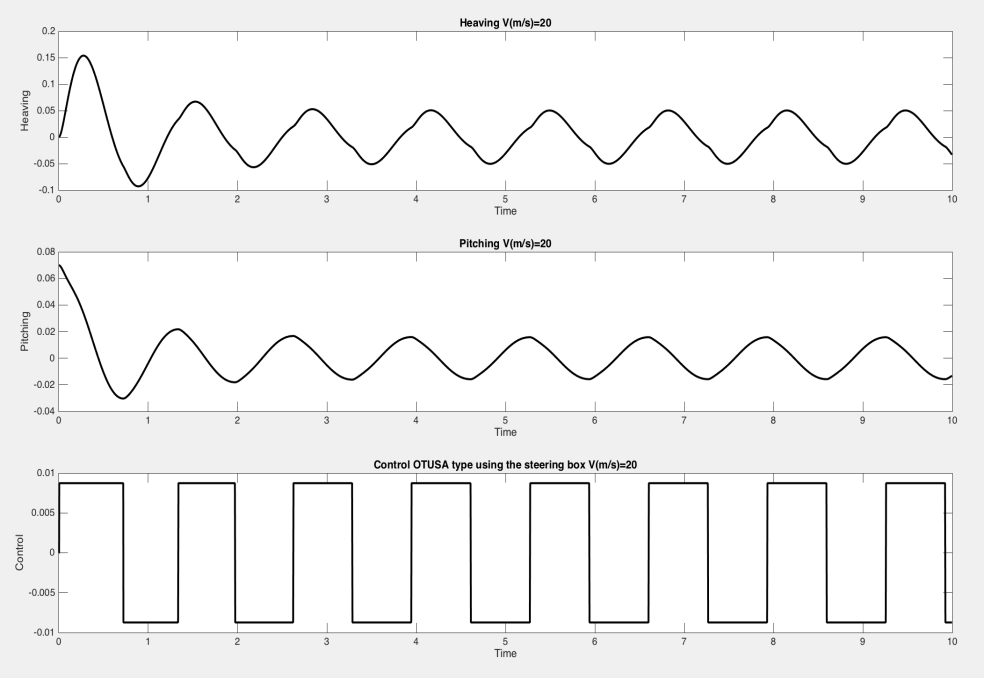

FIGURE 19. OTUSA control system. See also figure 17.

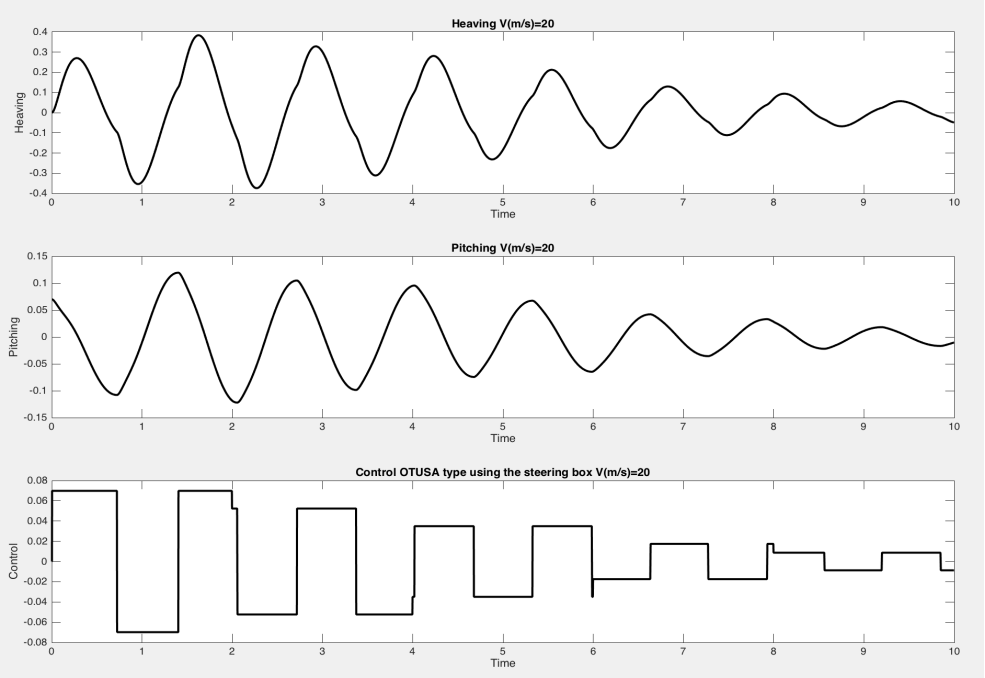

FIGURE 20. OTUSA's system. The magnitude of the control is reduced during the control process.

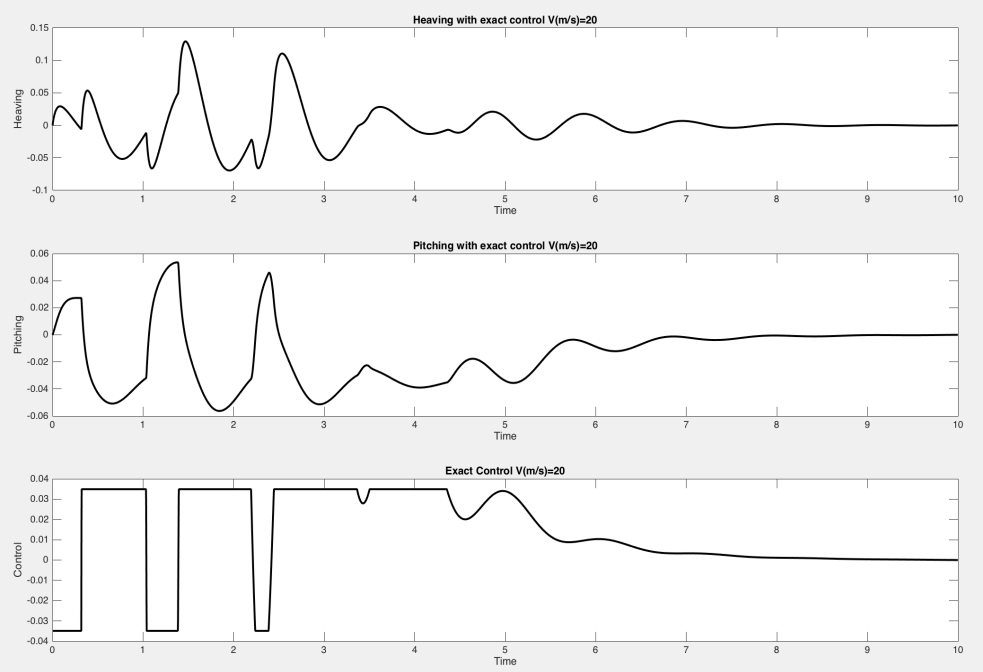

FIGURE 21. Exact control system with bounds on the control magnitude with the same perturbation as in the the two previous figures with OTUSA control system.

7. **Conclusion.** In this paper, we have suggested a formulation for a simple model in order to check the controllability of flying boats in a reduced configuration. In fact, only two degrees of freedom have been considered. The control law is derived from optimal control for a vanishing cost parameter ($\varepsilon \to 0$). The controllability is assumed using the theory of R. Bellman [1]. But a careful study has been necessary because the control system is a part of the stiffness and of the damping matrices. It has been explained and justified that both the rake angle and its time derivative are involved in the control process.
The optimal control laws found in subsections 6.1 and 6.4 are theoretical and can only be exactly applied as far as an electronic device coupled with a mechanical actuator, is used. The comparaison with the control system used by OTUSA shows the theoretical advantages of this exact control. But from a practical point of view, it is not obvious that these advantages would be significant. Because of the regulations in the America's cup, only mechanical devices can be used and the manufacturing of a mechanical system reproducing the exact control law is not discussed in this paper.
Therefore the strategy used by the American Team which is fully compatible with the rules, even if it is not optimal, is an interesting alternative. Nevertheless, much better results would be obtained by using slightly different manufacturing of the foil and the rudder. We do not explicit these improvements in this paper which are still to be discussed and checked. May be they will be discussed in a futur work.

Annex: the mechanical device used by OTUSA

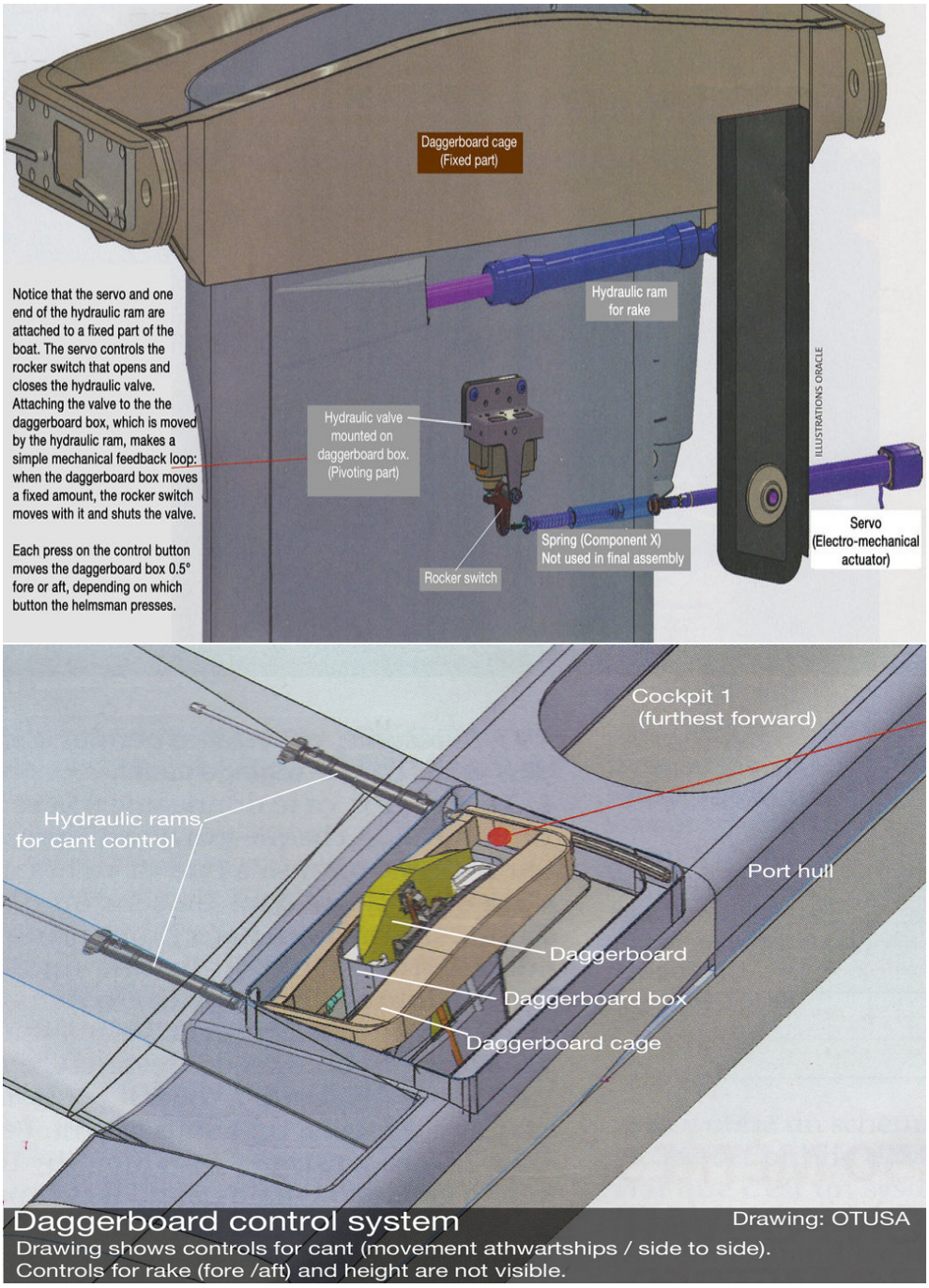

FIGURE 22. The Oracle USA-Team used this mechanical control to win the last eight races in a row. In particular, but not only, it enables them to navigate in the wake of the challenger mainly at the tacking [24].

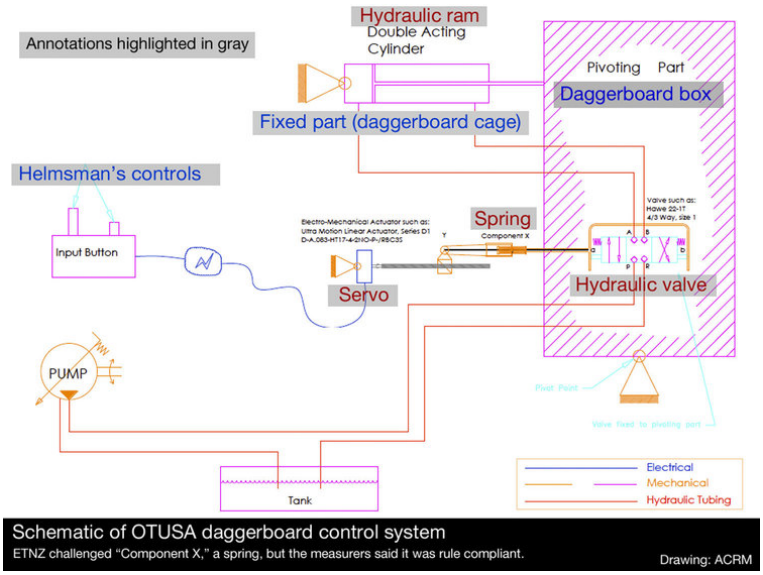

FIGURE 23. Principle of the device used published in [24]

References

[1] R. Bellman [1957], Dynamic programming, Dover edition.
[2] J.L. Lions, [1988] *Contrôlabilité exacte, perturbations et stabilisation de systèmes distribués*, Masson, Paris.
[3] Y.C. Fung, [1969], *An introduction to the theory of aeroelasticity*, Dover publication.
[4] E.H. Dowell, H.C. Curtiss Jr., R.H. Scanlan, F. Sisto [1978], *A Modern Course in Aeroelasticity*. Monographs and textbooks of solids and fluids. Alphen aan den Rijn, Sijthoff and Noordhoff International Publishers.
[5] Jean Cea [1968], *Optimisation, Théorie et Algorithmes*, Dunod, Paris.
[6] Ph. Destuynder [2007], *Introduction à l'aéroélasticité et à l'aéroacoustique*. Hermès-Lavoisier, Paris-Londres.
[7] Ph. Destuynder [2010], *Analyse et contrôle des équations différentielles*, Hermès-Lavoisier, Paris-Londres.
[8] Ph. Destuynder and M. T. Ribereau [1996], Non linear dynamics of test models in wind tunnels, in *Eur. J. Mech. A/Solids*,15,n°1, p. 91-136.
[9] $http://www.naiad.com/Product_Flyer_T - Foil.pdf$
[10] $http://www.marin.nl/web/Research - Topics/Motions/Ride - control - Foil - assist - craft.htm$
[11] $http://www.cupexperience.com/blog/2013/11/ac72 - foil - control - system - 2/$
[12] $http://www.boardrepair.co.uk/downloads/ConSysMoth.pdf$
[13] $http://www.gc32racing.com/foils/$
[14] $http://www.tandfonline.com/doi/abs/10.1080/14484846.2006.11464502$
[15] $http://dspace.mit.edu/handle/1721.1/42917$
[16] $http://dspace.mit.edu/bitstream/handle/1721.1/42917/245535660 - MIT.pdf?sequence = 2$
[17] $http://www.yachtingworld.com/blogs/matthew - sheahan/americas - cup - what - was - changed - on - oracle - 555$
[18] $http://news.mit.edu/2013/qaa - engineering - professors - on - americas - cup$
[19] Melina Freitag [20111], http://people.bath.ac.uk/mamamf/talks/ilas.pdf
[20] http://aerostudents.com/files/automaticFlightControl/stabilityAugmentationSystems.pdf
[21] http://contrails.iit.edu/DigitalCollection/1972/AFFDLTR72-063.pdf
[22] http://www.telegraph.co.uk/cars/columnists/andrew-english/sailing-the-ben-ainslie-americas-cup-yacht/
[23] https://www.quora.com/
[24] http://www.cupexperience.com/blog/2013/11/ac72-foil-control-system-2/